FUNCTION OF *LAZY1a* IN SILVER BIRCH (*Betula pendula*)

MSc. thesis

Sampo Muranen

University of Helsinki

Faculty of Biological and Environmental Sciences

Plant Molecular Biology

August 2019

HELSINGIN YLIOPISTO — HELSINGFORS UNIVERSITET — UNIVERSITY OF HELSINKI

Tiedekunta – Fakultet – Faculty Faculty of Biological and Environmental Sciences	Koulutusohjelma – Utbildningsprogram – Degree Programme Master´s Programme in Plant Biology	
Tekijä – Författare – Author Sampo Muranen		
Työn nimi – Arbetets titel – Title Function of *LAZY1a* in Silver Birch (*Betula pendula*)		
Oppiaine/Opintosuunta – Läroämne/Studieinriktning – Subject/Study track Plant Molecular Biology		
Työn laji – Arbetets art – Level MSc Thesis	Aika – Datum – Month and year 08/2019	Sivumäärä – Sidoantal – Number of pages 41

Tiivistelmä – Referat – Abstract

Tree shoot architecture research is important due to its significance in fields such as timber production, fruit and nut production and aesthetics of common areas. Also, research on genetic factors that regulate shoot and root system architecture might provide novel methods to store more carbon in forests and, hence, mitigate global warming in the future. *LAZY1* is one of the major genes that affects branch and tiller angle in herbaceous and woody species such as *Arabidopsis*, rice and peach tree. *LAZY1* has been under scrutiny over a decade but its molecular function remains unknown. However, it is known that *lazy1* mutation affects polar auxin transport. Here it is studied how LAZY1 affects initial branch angle, fiber length and reaction wood development in silver birch (*Betula pendula*). Also, transcript levels of few shoot architecture related genes were analyzed. *LAZY* phylogenetic analysis provided evidence of a duplication of LAZY1 in three studied tree species (*Betula pendula, Prunus persica, Populus trichocarpa*), duplicated genes are here named *LAZY1a* and *LAZY1b*. Plant material employed in this study was a segregating population (50:50) of back-cross 1 of weeping birch (*B. pendula* ´Youngii´) which has a truncated *lazy1a*. Histological samples of branches were prepared by cryo-sectioning, stained with carbohydrate binding Alcian Blue and lignin binding Safranin dyes to reveal patterns of tension wood development. Due to the large size of branch sections, samples were imaged with a microscope and the images were merged together in a Photoshop application. Branch angles were measured manually with a protractor (angle) tool from stem to the middle of a branch. The data was analyzed using mixed linear models due to the nature of used plant material. We could not use clones because of major issues in *in vitro* propagation. Branch samples were macerated, fibers imaged and measured by ImageJ software. *LAZY1a* gene expression levels were analyzed by RT-qPCR method. RNA-sequence analysis indicated that the expression pattern of *LAZY1a* and *LAZY1b* is similar in *B. pendula*. However, one should construct a promoter-reporter line to study with better resolution if their expression is spatially analogous. Initial branch angle was significantly different in wild type compared to *lazy1a* mutant. For future, one could generate single and double knock out lines of *lazy1a/b* to study if they have cumulative effect on the branch angle, an important factor in timber quality. Tension wood formation was difficult to quantify with the employed method, due to issues in segregating G-layered tension wood from thick-walled reaction wood. A chemical analysis of cellulose content might provide a more objective method to observe tension wood in branches. RT-qPCR method indicated that *LAZY1a* transcript levels are higher in wild type compared to mutant. A complementation or knock down experiment would provide sound evidence that *lazy1a* induces the weeping phenotype. X-ray diffraction method could be employed to study the orientation of cellulose microfibril angle in branches of the wild type vs. mutant. Generation of effective tensional stress requires a cellulose microfibril angle less than 10° and this angle is affected by auxin concentration. It is possible, that this angle is larger in *lazy1a* due to defect in polar auxin transport.

Avainsanat – Nyckelord – Keywords Silver birch, Betula pendula, reaction wood, tension wood, RT-qPCR, histology, LAZY1, tree, shoot architecture	
Ohjaaja tai ohjaajat – Handledare – Supervisor or supervisors Dr. Kaisa Nieminen, Prof. Ykä Helariutta	
Säilytyspaikka – Förvaringställe – Where deposited University of Helsinki e-thesis repository	
Muita tietoja – Övriga uppgifter – Additional information	

HELSINGIN YLIOPISTO — HELSINGFORS UNIVERSITET — UNIVERSITY OF HELSINKI

Tiedekunta – Fakultet – Faculty Bio- ja ympäristötieteellinen tiedekunta		Koulutusohjelma – Utbildningsprogram – Degree Programme Kasvibiologian maisteriohjelma
Tekijä – Författare – Author Sampo Muranen		
Työn nimi – Arbetets titel – Title *LAZY1* geenin vaikutus rauduskoivun varren ja oksien fenotyyppiin		
Oppiaine/Opintosuunta – Läroämne/Studieinriktning – Subject/Study track Molekulaarinen kasvibiologia		
Työn laji – Arbetets art – Level Maisterintutkielma	Aika – Datum – Month and year 08/2019	Sivumäärä – Sidoantal – Number of pages 41

Tiivistelmä – Referat – Abstract

Puiden varsien ja oksien arkkitehtuurin geneettisen säätelyn tutkimus on tärkeää, koska sillä on merkittävä vaikutus puutavaran tuotannossa, ruoan tuotannossa sekä koristepuiden jalostuksessa. Puiden geneettisen tutkimuksen tuottamalla tiedolla olisi myös mahdollista luoda uusia puulajikkeita, jotka ovat optimoituja hiilen sitomiseen. Näillä perinteisin menetelmin tai geneettisellä jalostuksella luoduilla puilla voisi olla tulevaisuudessa merkittävä osa ilmastonmuutoksen hillinnässä. *LAZY1* on merkittävä geeni, joka määrittää ruohovartisten kasvien (lituruoho, riisi) ja puiden (mm. persikka) arkkitehtuuria säätelemällä oksien ja varren kasvun suuntaa. LAZY1:n molekulaarista funktiota on tutkittu yli kymmenen vuotta. Tiedetään, että LAZY1 osallistuu polaariseen auksiinin kuljetuksen, mutta proteiinin toimintamekanismia ei vielä tunneta. Tässä tutkielmassa on tutkittu LAZY1:n vaikutusta rauduskoivun (*Betula pendula*) oksien kasvukulmaan, kuitujen pituuteen ja reaktiopuun muodostumiseen. Tämän lisäksi muutamia puuarkkitehtuuriin mahdollisesti vaikuttavien geenien ekspressiota on mitattu RT-qPCR menetelmällä. *LAZY* geeniperheen fylogeneettinen analyysi antoi viitteitä siitä, että tarkastelluissa puulajeissa (*Betula pendula, Prunus persica, Populus trichocarpa*) on tapahtunut duplikaatio *LAZY1*-geenissä, joita kutsutaan tässä tutkielmassa termein *LAZY1a* ja *LAZY1b*. Käytetty kasvimateriaali oli segregoiva BC1 takaisinristeytyspopulaatio, jossa 50%:ssa kasveista oli oletettu *lazy1a* mutaation aiheuttama riippuva fenotyyppi. Histologiset näytteet valmistettiin cryotomilla ja näytteet värjättiin hiilihydraatteihin sitoutuvalla Alcian sininen ja ligniiniin sitoutuvalla Safraniini -väreillä. Oksanäytteet olivat suuria normaalia mikroskooppityöskentelyä varten, joten lopulliset kuvat täytyi koota kuvankäsittelyohjelmalla useasta kuvasta. Oksien kasvukulma mitattiin astemittarilla ja data analysoitiin lineaarisella sekamallilla, koska analyysissä täytyi ottaa huomioon osapopulaation eri yksilöiden geneettinen vaihtelu tekijänä. Oksanäytteitä maseroitiin ja kuidut kuvattiin ja mitattiin ImageJ-ohjelmiston avulla. Data aiemmasta RNA-sekvenssianalyysistä osoitti, että *LAZY1a:*n ja *LAZY1b*:n ekspressioprofiili on samankaltainen rauduskoivussa. Tätä voisi tutkia lisää promoottori-GFP-reportteri konstruktiolla, jolla näkisi paremmalla resoluutiolla, ekspressoituvatko geenit samassa solukossa samaan aikaan. Oksien kasvukulma erosi tilastollisesti merkittävästi villityypissä verrattuna *lazy1a* mutanttiin. Tulevia tutkimuksia varten olisi tärkeää luoda *lazy1a/b* tuplamutanttilinja ja tarkastella, onko näillä geeneillä kumulatiivista vaikutusta oksien kasvukulmaan, joka on merkittävä tekijä puutavaran tuotannossa. Vetopuun muodostumista oli hankala mitata käytetyllä menetelmällä, koska kuvista ei aina erottanut, mikä on selluloosarikasta vetopuuta. Kemiallinen analyysi selluloosan mittaamiseksi olisi tässä tapauksessa mahdollisesti objektiivisempi menetelmä. RT-qPCR metodi osoitti, että *LAZY1a:n* transkriptiä on enemmän villityypissä kuin mutantissa. Geenin komplementointi tai mutatointi -koe osoittaisi, että *lazy1a* aiheuttaa kyynelkoivun oksien riippuvan fenotyypin. Röntgendiffraktiolla olisi mahdollista tutkia selluloosasäikeiden sijoittumista soluseinään. Säikeiden alle 10 asteen orientaatiolla on olennainen osa vetolujuuden synnyttämisessä puusolukossa ja auksiinin konsentraation oletetaan vaikuttavan selluloosan sijoittumiseen soluseinässä. On siis mahdollista, että selluloosakuitujen kulma on liian iso kyynelkoivussa, mistä johtuu puun riippuva fenotyyppi.

Avainsanat – Nyckelord – Keyw ords
Rauduskoivu, Betula pendula, reaktiopuu, vetopuu, RT-qPCR, histologia, LAZY1, puun arkkitehtuuri

Ohjaaja tai ohjaajat – Handledare – Supervisor or supervisors
Kaisa Nieminen, Ykä Helariutta

Säilytyspaikka – Förvaringställe – Where deposited
Helsingin yliopiston e-thesis opinnäytteet

Muita tietoja – Övriga uppgifter – Additional information

TABLE OF CONTENTS

Abbreviations

At - *Arabidopsis thaliana*
ARF19 - AUXIN RESPONSIVE FACTOR 19
ARK2 - ARMADILLO REPEAT KINESIN 2
Bp - *Betula pendula*
$Ca2^{+}$ - Calcium Ion
cDNA - Complimentary DNA
CO_2 - Carbon Dioxide
CTAB - Cetyl Trimethylammonium Bromide
Ct - Cycle threshold
EDTA – Ethylenediaminetetraacetic Acid
EtOH - Ethanol
GC% - Guanine Cytosine percentage
GFP - Green Fluorescent Protein
G-layer - Gelatinous layer
GOI - Gene of Interest
HCl - Hydrochloric Acid
H^{+} - Proton
IAA5 – INDOLE ACETIC ACID 5 (auxin signaling repressor)
LiCl – Lithium Chloride
IPCC - International Panel for Climate Change
NaCl – Natrium Chloride
N_2 - Molecular Nitrogen
PIN3 - PIN-FORMED 3
Pp - *Prunus persica*
Pt - *Populus trichocarpa*
PVP - polyvinylpyrrolidone
RNAi - RNA interference
RT-qPCR - Reverse Transcriptase Quantitative Polymerase Chain Reaction
S-layer - Secondary Cell Wall Layer
STD - Standard Deviation
TAIR - The Arabidopsis Information Resource
Tm - Melting Temperature
TRIS - Tris(hydroxymethyl)aminomethane
T-test - Student´s T-test
TAC1 - TILLER ANGLE CONTROL 1
WOX4 - WUSCHEL RELATED HOMEOBOX 4
Zm - *Zostera marina*
35S - Promoter used for constitutive gene expression

1 INTRODUCTION

1.1 Importance of Tree Shoot Architecture Research

Interest in tree shoot architecture research has been increasing in the past decades because it has a major socioeconomic impact in various fields such as forestry, landscape management, aesthetics and industrial fruit production (Dardick *et al.,* 2013). Tree related industry including fruit trees, nut trees and forest products are a major economic factor worth 225 billion dollars in the United States alone (Hill and Hollender, 2019). In ecological terms, columnar phenotype apple trees consume only 50% of the water compared to ordinary cultivars during growing season (Jacob, 2010). Tree shoot architecture research is of special interest in the tree orchard business where chemical growth regulation, pruning, manual branch angle control and grafting are major expenses (Hill and Hollender, 2019). Also, tree shoot architecture research is important in timber industry because branch angle, number and diameter has a considerable impact on timber quality (Niemistö *et al.,* 2008: 184).

Unless there will be a major change in current dietary trends, world food production should roughly double by 2050 due to the growing world population, change in dietary habits and use of farmland for bioenergy crop production (Foley *et al.,* 2011). Therefore, it is imperative to develop means to produce more food on less farmland. Tree shoot architecture research is essential in this development. For instance, it is predicted that the use of columnar apple varieties could raise yield over 3-fold compared to ordinary varieties (Jacob, 2010, Dardick *et al.,* 2013).

Global warming is probably the most alarming environmental issue of the current era. According to the recent IPCC report, limiting global warming to 1.5°C would require immense land use change, among other major transitions in energy use and infrastructure (IPCC, 2018). This should motivate tree shoot architecture research since trees pose an inexpensive method of capturing CO_2 from the atmosphere. According to Cernansky (2018), there are 2 billion hectares of deforested or degraded land available for tree planting worldwide. This translates to roughly twice the size of Sahara. A feasible method to enhance carbon capture and produce valuable timber by a given area could be either conventionally or molecularly bred trees with altered shoot architecture.

High density tree planting might provide a method for boosting timber production and carbon capture. Currently this is not practical because trees respond to shading by growing taller but thinner (Mann & Plummer, 2002). A solution to this is redesigned biological pathways that lead to short and nearly branchless stems that display little response to shading (Mann & Plummer, 2002). Another question is whether high density forests would make sense in ecological terms. Rebuilding forests require broad approaches in questions such as water availability, soil condition, biodiversity, food chains etc. (Cernansky, 2018). Thus, high density forests should be trialed carefully before extensive planting.

Growth and development of shoots into tree crown is a complex and flexible process. The mechanisms involved are currently poorly known (Dardick *et al.,* 2013). These mechanisms include genetic interactions with environmental factors such as light, wind and gravity. Also, pressure exerted on cells, nutrition, phytohormones, cell size, cell proliferation and cell wall chemistry contribute to tree shoot architecture (Hill and Hollender, 2019). To be able to implement judiciously tree related genetic information we must know the underlying mechanisms more thoroughly.

1.2 Silver Birch as a Model Organism

The genus of birch (*Betula*) belongs to the family of *Betulaceae*. *Betula* species are deciduous hardwood trees, located in the northern hemisphere and characterized by vast morphological variation (Niemistö *et al.,* 2008). Typical for *Betula* genus are wind pollinated and monoecious flowers (Niemistö *et al.,* 2008).

Employing a tree species as a model organism in genetic studies poses a challenge in contrast to annual plants such as *Arabidopsis thaliana*. This is due to several years long juvenile stage which trees usually require before they start to flower and subsequently enable crossings (Longman & Wareing, 1959). Conveniently, silver birch can be induced to flower within a year when introduced into special accelerated flowering conditions: long-day illumination with elevated CO_2 and temperature levels (Longman & Wareing, 1959).

Silver birch (*Betula pendula*) has a diploid (2n = 28) 440 Mbp genome (Salojärvi *et al*., 2017). Chromosome number (ploidy) in *Betula* species is highly variable; it spans from 2 in *B. Pendula* and

a few others to 12 in *B. gynoterminalis* (Ashburner *et al*., 2013). Assembling polyploid plant genomes has been difficult due to at least two reasons: First, it is difficult to separate relatively similar subgenomes from one to another. Second, plant genomes commonly harbor active retrotransposons which cause a copy-and-paste effect within homologous chromosomes causing erratic extensions (Ming & Man Wai, 2015). For these reasons diploid silver birch is an ideal woody plant for molecular genetic studies.

1.3 Premature Stop Codon in *Betula pendula* ´Youngii´ *LAZY1*

Betula pendula `Youngii´ cultivar originates from Central Europe and is a common ornamental birch with a dome-shaped crown (Fig 1A). During the recent birch genome sequencing project it was learnt that a ´Youngii´ birch, growing in Helsinki University Viikki campus site has a premature stop codon in *BpLAZY1* gene (Fig 1B) (Salojärvi *et al*., 2017). LAZY1 protein is known to affect tiller angle in rice (Li *et al*., 2008). Also, in plum tree (*Prunus domestica*) *lazy1* mutation induces a pendulous growth habit (Hill & Hollender, 2019). For these reasons, it was hypothesized that *lazy1* induces the weeping phenotype in ´Youngii´ birch. Mutated *LAZY1* is referred hereafter as *lazy1a* because there are at least two *LAZY1*-like genes in silver birch genome.

Figure 1. (A) *Betula pendula* ´Youngii´ (left) and *Betula pendula* (right) at Helsinki University Viikki campus site. **(B)** LAZY1a contains a point mutation (131C>A) transforming the TCG (Serine) codon into a premature TAG stop codon (Salojärvi *et al., 2017)*.

Still, further evidence is required to unambiguously display that *lazy1a* induces the weeping phenotype in silver birch. Due to the time constraints of this project, a transgenic line complementing or knocking down *LAZY1a* could not be established. Also, all commercially propagated *B. pendula* ´Youngii´ trees probably originate from the same mutant individual, thus they are not expected to harbor alternative *lazy1a* knock-out/knock-down alleles. Therefore, we are aiming at sequencing the

closest orthologue of *LAZY1a* from a weeping grey alder (*Alnus incana* ´Pendula´) belonging to the *Betulaceae* family. If *LAZY1a* is also mutated in the weeping gray alder, this would provide further evidence that *lazy1a* induces the weeping phenotype in silver birch.

1.3.1 LAZY1 and Gravitropism

LAZY1 has been under scrutiny in agronomic research due to its significance in rice tiller angle control. Li *et al.* (2008) have argued that LAZY1 negatively controls basipetal (shoot to root) auxin transport and thereby regulates gravitropism in rice. Gravitropism is explained by a century old starch-statolith hypothesis. In this theory gravity is sensed by sinking of high-density amyloplasts in statocytes, the gravity perceiving cells (Haberlandt, 1900; Taniguchi *et al.*, 2017). These cells are located in the endodermis of *Arabidopsis* shoots (Fukaki, *et al*., 1998; Taniguchi *et al.*, 2017). In poplar stem, statocytes are first located in the endoderm (most inner layer of cortex) and after the loss of endodermis, statocytes are positioned in secondary phloem (Gerttula *et al.,* 2015).

Subsequently to statolith sinking, a signal is converted by an unknown mechanism into auxin flow towards gravity by PIN3 auxin efflux carrier proteins (Taniguchi *et al.*, 2017). According to a current theory, auxin flow leads to a decrease in apoplastic pH, hence the name acid growth hypothesis. Acidification is due to auxin induced activation of plasma membrane bound proton pumps, tonoplast bound Ca^{2+}/H^{+} antiporters and transcriptional induction and/or activation of cell wall modifying genes/enzymes such as expansins, xyloglugan endotransglucosylases/hydrolases and polygalacturonases. Further on, lower apoplastic pH allows diffusion of auxin into the symplast because in lower pH, negatively charged auxin gains a proton and is able to diffuse through the nonpolar plasma membrane. Also, lower pH causes pectin de-methylation which itself decreases pH. Loosening of the cell wall matrix structures and turgor pressure then increases cell volume in a coordinated manner (Reviewed by Arsuffi & Braybrook, 2018).

According to Taniguchi *et al.* (2017) *Arabidopsis* LAZY1, LAZY2 and LAZY3 proteins are redundantly responsible for gravitropic response downstream of amyloplast sedimentation in statocytes. The authors have displayed that *LAZY2* and *LAZY3* genes are expressed in root columella cells (root gravitropism) but *LAZY1* is not. The authors have also discovered that LAZY1 has the strongest impact on shoot architecture from the *LAZY*-clade, yet, its molecular function remains elusive.

During the ´Youngii´ project it was discovered that the *lazy1a* birches had very poor root growth in *in vitro* propagation making cloning virtually impossible. This provided major challenges due to shortage and heterogeneous plant material. However, poor root growth in *lazy1a* birches is possibly connected to reduced LAZY1a expression and may therefore be an interesting phenomenon for future studies of its molecular function in tree species.

1.4 Reaction Wood

Trees have a spectacular capacity to maintain vertical growth in the main stem under harsh environmental conditions such as weight, wind, gravity and bending due to uneven ground (Barnett *et al.,* 2014: 2). According to the current dogma, maintaining upward growth in stems is possible due to a specialized cell type - reaction wood - which is further classified into compression wood and tension wood (Barnett & Jeronimidis 2003: 118). Angiosperm trees form tension wood (Fig 2A) which creates tensile force that pull stems and branches away from the gravity vector. Vice versa, gymnosperm trees form compression wood (Fig 2B) which produces a pushing force bending branches and stems against gravity (Reviewed by Du & Yamamoto, 2007).

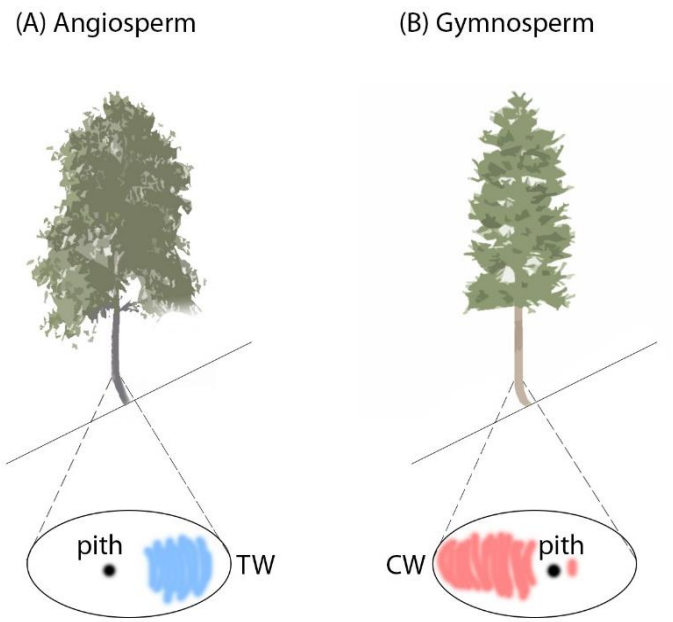

Figure 2. Reaction wood formation in angiosperm and gymnosperm trees. Reaction wood forms when plants are under growth stress such as uneven ground and consequent strain in stem. (**A**) In angiosperm trees, tension wood (TW) forms to the side with tensional stress. **(B)** Compression wood (CW) forms in gymnosperms to the side with compressional stress. Adapted from Gril *et al*. (2017).

1.4.1 Reaction Wood and Cell Wall Composition

Reaction wood formation changes plant cell wall chemical composition. For instance, the amount of lignin is increased in compression wood while polysaccharides abate (Fagerstedt *et al.,* 2014: 38). In contrast, tension wood contains less lignin and its deposition is different compared to

compression wood: lignin is polymerized mainly in middle lamellae and in primary cell walls. In compression wood lignin is mainly deposited in the secondary cell wall. Further on, tension wood often contains a gelatinous layer (G-layer) (Fagerstedt *et al.,* 2014: 37). G-layer is also called the tertiary cell wall layer that contains mostly cellulose and little lignin (Gerttula *et al.,* 2015). However, depending on species, tension wood cell wall anatomy is highly variable. It may contain a G-layer, multilayered secondary cell wall or a cell wall that is similar to normal fibers (Fig 3).

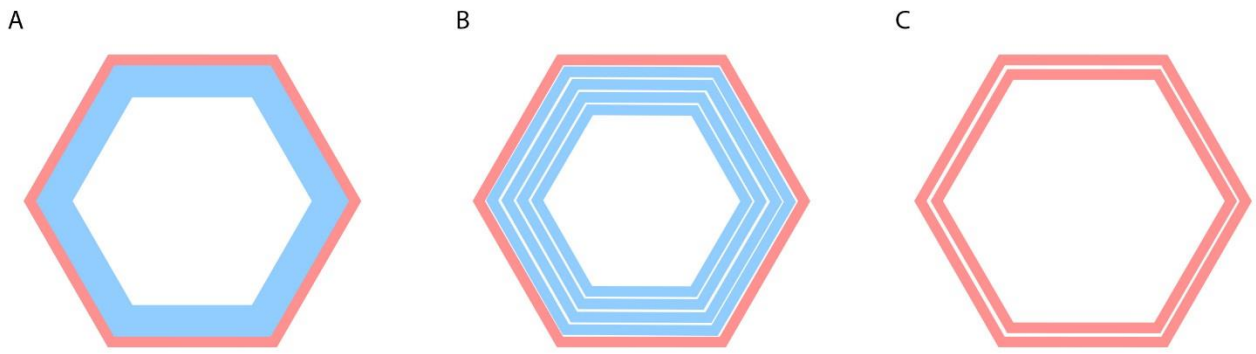

Figure 3. Tension wood structure in three tropical angiosperm species. G-layers are indicated with blue, secondary cell walls are indicated with red. **(A)** *Eperua falcate* displays thick walled G-layer. **(B)** Multi-laminate structure of G-layers in *Laetia procera.* **(C)** *Simarouba amara* tension wood does not vary from normal secondary cell wall structure. Modified from Ruelle (2014: 25).

1.4.2 Force Generation in Tension Wood

The mechanism how G-layers are able to produce pulling force is being debated. G-layers are not attached to the surrounding cell walls (Barnett *et al.,* 2014: 8), thus making tensile force transmission to the surrounding tissue somewhat unexplained. However, an enzymatic removal of the G-layer has been demonstrated to elongate the surrounding S-layer by 1,6% indicating its importance in creating tensile force (reviewed by Mellerowicz & Gorshkova, 2011). A model has been proposed for G-layer tensile force generation which involves a network of crystalline cellulose (Fig 4). G-layers have high cellulose content and because cellulose is hydrophilic, G-layers are absorbing water. This causes lateral swelling and, hence, inward force and axial shrinkage of the G-layer network (Mellerowicz & Gorshkova (2011).

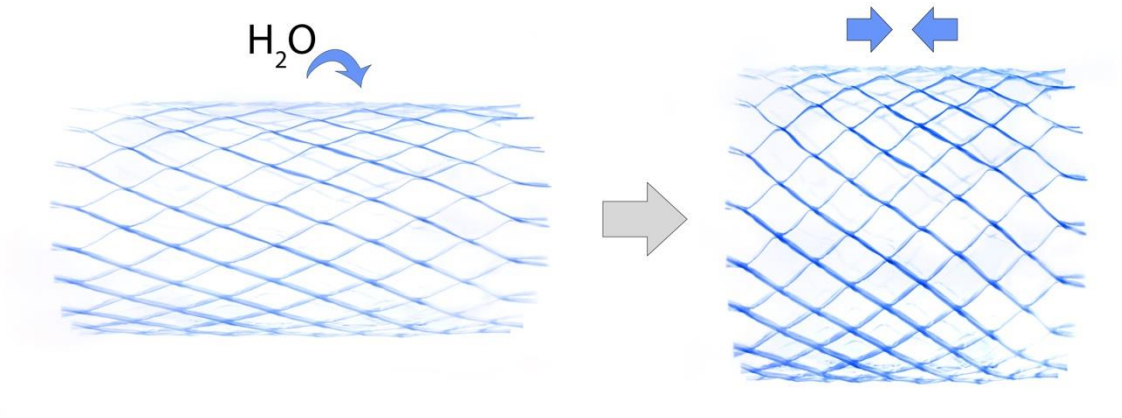

Figure 4. Force generation in tension wood. According to the shrinking network model force generation in tension wood tissue is induced by intake of H_2O by tissue containing mostly of hydrophilic cellulose. Consequently the network shrinks and produces tensional force that pulls the opposite ends of the cellulose network towards each other. Adapted from Mellerowicz & Gorshkova (2011).

1.4.3 Tension Wood Formation in *lazy1a B*ranches

Involvement of auxin in reaction wood formation is debated in the literature (reviewed by Tocquard *et al.,* 2014: 118-119). However, gene expression in auxin signaling pathway has been displayed to alter after stem bending experiments. Transcription of two AUX/IAA genes (repressional transcription factors) was altered in tension wood tissue compared to opposite wood in poplar (Moyle *et al.,* 2002, Tocquard *et al.,* 2014: 118-119). As explained previously, LAZY1 functions upstream of PIN3 which directs auxin efflux towards gravity. Due to the placement within endodermis (later in phloem) and gravistimulation, PIN3 is aligned in a manner that directs auxin efflux towards the cambial zone in the upper part of the stem and towards the cortex on the lower side (Gerttula *et al.*, 2015). Therefore, it has been hypothesized here that tension wood development might be affected in *lazy1a* branches.

1.5 Adaxial and Abaxial Fiber Length in *lazy1a* Branches

According to Gerttula *et al.* (2015), our current knowledge on gravitropism stems from studies conducted on herbaceous species. Herbaceous species supposedly react to gravitational pull by asymmetric cell elongation (acid growth hypothesis) while lignified woody cells cannot expand. Therefore, woody species react to gravitational cue by another mechanism, which is asymmetric

secondary growth (Gerttula *et al.,* 2015). In asymmetric secondary growth cell division rate is increased in parts of the vascular cambium leading to elliptical shape in cross sections of stems and branches (Gerttula *et al*., 2015).

As explained previously, auxin has long been thought to induce cell expansion through the mechanism explained by acid growth hypothesis. Björklund *et al.* (2007) demonstrated that auxin is together with gibberellins enhancing stem growth in hybrid aspen (*Populus tremula x tremuloides*). According to Nilsson *et al.* (2008), fiber and vessel dimensions are controlled by auxin. Their research indicated that in transgenic lines with reduced auxin responsiveness, xylem cells were smaller in diameter and shorter compared to wild-type cells in stems. Here, it is assumed that the mechanism controlling auxin flow towards cambium on top and towards cortex on bottom side of branch might be compromised in ´Youngii´ birch due to the *lazy1a* mutation. This might have an effect on average fiber length. Therefore, adaxial and abaxial xylem from wild type and mutant branches were macerated and fiber lengths were measured.

1.6 RT-qPCR Gene Expression Analysis in Adaxial and Abaxial Flanks of Branches

To verify that *LAZY1a* transcript levels are lower in mutant than in wild type trees, *LAZY1a* transcript levels were analyzed by RT-qPCR. Also, expression levels of few tree architecture candidate genes (Table 1) were compared between wild type and mutant.

Table 1. Genes of Interest in RT-qPCR Analysis

GOI	Function	Reference
LAZY1a	branch growth upwards	Taniguchi *et al*., 2017
ARK2	fiber maturation	Gerttula *et al.,* 2015
ARF19	auxin signaling	Immanen *et al*., 2016
WOX4	phloem activity	Suer *et al.,* 2011
PIN3	auxin efflux	Friml *et al.,* 2002
PHOT1	phototropism	Christie *et al*., 1999

2 AIMS OF THE STUDY

Identifying the biological function of LAZY1a in silver birch (*Betula pendula*) was the main objective in this project. This aim was pursued by comparing samples of wild type silver birch (*Betula pendula*) and *lazy1a* mutant (*Betula pendula* ´Youngii´) branches. Primary hypothesis was that the weeping birch lacks or deposits tension wood in its branches erratically. Another area of interest was whether *LAZY1a* impacts fiber growth. Identifying genetic factors that affect fiber physical dimensions is important in tree breeding because fiber length has major impact on different wood products quality such as paper strength. Third objective was to study branch angle because steep branch angle causes issues in timber quality. Research on *LAZY* gene family might provide useful insights in breeding trees with optimal branch angle. Last objective has been to study interactions of *LAZY1a* and few other candidate genes that might influence tree shoot architecture.

3 MATERIALS AND METHODS

3.1 Plant Material, Growth Medium and Growth Conditions

Used plant material was a segregating population of backcross 1 (BC1). Wild type phenotype of F1 generation was backcrossed using pollen from *Betula pendula* ´Youngii´. 100 individuals were grown of which 55% were wild type and 45% were mutant phenotype.

Plants were grown in peat:sand:vermiculite (6:2:1) and fertilized with granular Osmocote Exact (Everris) 2 g/liter of growth medium. Trees were grown in 3-liter pots on a growth table in Viikki campus greenhouse under ambient light and temperature conditions for over two growing seasons.

3.2 *LAZY1* and *LAZY2* Phylogenetic Tree and Amino Acid Alignment

Amino acid sequences of *LAZY1*, *LAZY2* and *LAZY3* genes were retrieved from the *Arabidopsis* Information resource (www.tair.org) database. These sequences were used to identify the closest paralogs in the *Betula pendula* genome. Best matching hits were *LAZY1a* and *LAZY1b* for *LAZY1* and *LAZY2* for *LAZY2*. *Arabidopsis LAZY3* provided only duplication hits in the studied species, therefore it has been left out from the phylogenetic tree

Amino acid sequences of *Betula pendula LAZY1a* and *LAZY1b* and *Arabidopsis thaliana LAZY1*, *LAZY2* were uploaded to Phytozome v12.1 and the most significantly similar sequences were collected from the species studied (Table 2). Duplicates were removed and sequences were copy-pasted to MEGA7 program (Kumar, Stecher & Tamura, 2015). An alignment was constructed using default settings in CLUSTAL algorithm. Manual curation was conducted and the phylogenetic tree was constructed using maximum likelihood method with JTT+G+I settings and bootstrapping (1000 replications).

Table 2. Genes Used in Phylogenetic Analysis

GOI	Species	Ascension number
AgLAZY1	*Alnus glutinosa*	NA
AtLAZY1	*Arabidopsis thaliana*	At5G14090
AtLAZY2	*Arabidopsis thaliana*	At1G17400
BpLAZY1a	*Betula pendula*	Bpev01.c0052.g0076.m0001
BpLAZY1b	*Betula pendula*	Bpev01.c0566.g0022.m0001
BpLAZY2	*Betula pendula*	Bpev01.c0045.g0042.m0001
OsLAZY1	*Oryza sativa*	Os11g29840.1
OsLAZY2-1	*Oryza sativa*	Os07g42290.1
OsLAZY2-2	*Oryza sativa*	Os09g26840.1
OsLAZY2-3	*Oryza sativa*	Os03g29270.1
PtLAZY1-1	*Populus trichocarpa*	Potri.003G168700.1
PtLAZY1-2	*Populus trichocarpa*	Potri.001G327500.2
PtLAZY1-3	*Populus trichocarpa*	Potri.001G059100.1
PtLAZY2-1	*Populus trichocarpa*	Potri.003G068300.1
PtLAZY2-2	*Populus trichocarpa*	Potri.001G166700.1
PtLAZY2-3	*Populus trichocarpa*	Potri.006G140100.1
PpLAZY1-1	*Prunus persica*	Prupe.3G308500.1
PpLAZY1-2	*Prunus persica*	Prupe.1G222800.2
PpLAZY2-1	*Prunus persica*	Prupe.7G195900.1
PpLAZY2-2	*Prunus persica*	Prupe.3G038300.1
ZmLAZY1	*Zostera marina*	Zosma225g00060.1
ZmLAZY2-1	*Zostera marina*	Zosma176g00170.1
ZmLAZY2-2	*Zostera marina*	Zosma59g00310.1

3.2 Reaction Wood Deposition

Before samples were cut, topside of the branch was marked with a permanent marker. Subsequently, 1 cm long pieces were cut and samples were placed in an ice bath and then stored at -20°C. Cryotome sections were cut with LEICA CM3050S, each sample being 25 microns thick. After a successful sample was obtained, the topside of the sample which was standing on the holder, was marked by cutting. This provided a reference point and, therefore, aided later in microscopy to

identify the topside of the branch. Samples were then hydrated with a drop of dH_2O and stained with 0,05% Safranin in 50% EtOH. Excess Safranin was washed away with dH_2O. Samples were then stained with 1% Alcian Blue. Excess stain was washed away with dH_2O. Samples were imaged within an hour with Leica2500 DM light microscope. Due to the large size of branch sections, whole sections were constructed from multiple images using Photoshop v.20.0.1 photo merge tool with default settings.

3.3 Xylem Fiber Length Measurements

Length of xylem fibers were measured from 5 wild type and 5 mutant branches (Table 3). Cut samples were cooled in an ice bath and subsequently stored in -20°C. After thawing, samples were debarked and placed in 30% hydrogen peroxide and glacial acetic acid (1:1) solution and kept at +56°C for 50 h. Samples were then washed 3 times and vortexed extensively to separate fibers from each other. 100 µl from each sample tube was then pipetted on a glass slide and imaged with Leica2500 DM light microscope at 10x magnification. Fiber lengths were measured using ImageJ 1.47v program.

Table 3. Branch Samples in Fiber Length Experiment

Tree ID	Sample length (cm)	Distance from stem (cm)	Sample diameter (mm)	Branch length (cm)
WT 9_4	1	4	2,6	40,5
WT 9_6	1	5,5	2,7	44
WT 9_10	1	4	2,8	40
WT 9_19	1	5,5	2,8	50
WT 9_83	1	4,5	2,7	42
M 9_1	1	3,5	2,7	33
M 9_2	1	5	2,9	28
M 9_3	1	3,5	2,8	26
M 9_70	1	3,5	2,3	33
M 9_79	1	2,6	2,7	50

3.4 Branch Angle Measurements

Branch angles were measured manually from 3 normal, 3 intermediate and 3 mutant phenotypes using a protractor tool. Angle was measured clockwise between stem and middle of a branch. Measurements were performed in February 2018 while the trees were dormant after 1 growing season.

3.5 Candidate Gene Expression Analysis by RT-qPCR

RNA extraction, DNase and cDNA synthesis

Branch samples were collected from 3 wild type and 3 mutant trees. Samples were cut through the pith resulting in adaxial and abaxial flanks which were snap frozen in liquid nitrogen. Due to a malfunction in the -80°C freezer, samples were stored at -20°C for 10 days until RNA was extracted. A modified version of a pine tree RNA extraction method (Chang *et al.,* 1993) was employed. First, samples were pulverized in liquid N_2 and then ~100 mg was spooned into a 2 ml Eppendorf tube containing 750 µl of pre-warmed (65°C) extraction buffer (Table 4) and 15 µl of β-mercaptoethanol.

Table 4. RNA Extraction Buffer

Amount	Substance
10 g	2% CTAB
50 ml	100 mM Tris-HCL pH 8.0
25 ml	25 mM EDTA
200 ml	2 M NaCl
10 g	2% PVP
~205 ml	dH_2O
500 ml total volume	

Suspension was vortexed and left to incubate for 3 minutes at 65°C in a heat block. After incubation, 750 µl of chlorophorm:isoamylalcohol (24:1) was added and tube was mixed manually for 30 seconds. Phases were then separated by centrifuging (13000 rpm) at room temperature for 10 minutes. Subsequently, upper layer was pipetted into a new tube containing 750 µl of chlorophorm:isoamylalcohol (24:1) and mixed manually for 30 seconds. Phases were separated by centrifuging (13000 rpm) at room temperature for 10 minutes. 600 µl of upper layer was pipetted into a new 1,5 ml Eppendorf tube containing 150 µl of 10 M LiCl. RNA was then precipitated by storing the samples at +4°C overnight. Samples were centrifuged (13000 rpm) for 15 minutes at +4°C. Supernatant was poured away and the RNA was washed with 70% EtOH. EtOH was evaporated completely at room temperature in a fume hood. Subsequently RNA pellet was dissolved in 200 µl of dH_2O. Samples were stored at -20°C for a month.

Due to issues with genomic DNA contamination on test gel runs, nucleotide concentration was diluted to ~200 ng / µl. Nucleotide concentration was measured with Nanodrop. DNase treatment was conducted according to Promega RQ1 RNase-Free DNase (#M6101) protocol. First strand cDNA synthesis was conducted according to Thermo Scientific protocol (#K1612) with 100 ng of RNA loaded into each reaction tube. cDNA synthesis was conducted by the following program: 5 min at +25°C, 60 min at +37°C and 5 min at +70°C. Samples were then stored at -20°C for 3 months.

Primer Design and Primer Efficiency Experiment

First, amino acid sequences of the GOIs were looked up from The Arabidopsis Information Resource (TAIR) database. These amino acid sequences were then uploaded to the birch genome database and the most significantly similar matches were chosen for further analysis. Primers were designed to span over introns to avoid genomic DNA contamination in the qPCR run. Exon sequences were uploaded on www.Primer3Plus.org (Untergasser *et al.,* 2007) and primers were picked with default settings. The first few resulting primers were compared to the exon data. 2-3 primers were selected and primer efficiency was calculated for one primer per GOI (Table 5).

Table 5. Primer Pairs Designed for GOIs

GOIs F/R primer	5´ PRIMERS 3´	Tm (°C)	GC%	P. Len (bp)	Primer efficiency	Reference
1.1 ACTIN7_F	CACCACTGCTGAGCGGGAAA	62,4	60	100	2,009785579	
1.2 ACTIN7_R	GGGCAACGGAACCTCTCAGC	63,8	65			
4.1 UBG_F	CAGCGTCTCCGCAAGGAGTG	63,1	65	128	1,975646587	
4.2 UBG_R	TAATCACCGCCGGCCTTCTG	62,2	60			
5.1 PP2A_F	GGAGGATAGGCATTGGAGAG	56,5	55	213	1,951158791	Sutela *et al.*, (2011)
5.2 PP2A_R	CTGCATCACGGATCGAGTAA	63,8	50			
6.1 LAZY1a_F	GGTTGGATGCATCGTAAGTTCC	58	50	88	1,929031273	
6.2 LAZY1a_R	ACTGTTGATCGTCAACCGATG	56,3	47,6			
11.1 ARK2_F	GCCCAAAGATGCCAGACAA	57,6	50	93	1,897659505	
11.2 ARK2_R	TCAGCCAATGCCACCTTT	56,1	50			
13.1 TAC1_F	CCGTTCTTCGAACCAAACAT	54,5	45	180	NA	
13.2 TAC1_R	CGCCATTGGTGATAAATCCT	53,9	45			
15.1 PIN3_F	GCCTCACTTGGTCTCTAGTCTCTT	59,5	50	87	1,840737745	
15.2 PIN3_R	CTGCATCCGACAGTATGGAA	55,9	50			
19.1 ARF19_F	GCATGCAGATCAACTTTGGA	54,7	45	177	2,011190915	
19.2 ARF19_R	TTTCAGTACCTCGTCGAGCA	57,3	50			

22.1 WOX4_F	CTTCATCCGACCCGAAAGT	56,2	52,6	157	1,839756694	
22.2 WOX4_R	GCGCATTCCTCCCTTATACA	56,4	50			
24.1 PHOT1_F	GGTTACACATCCAAAGAGGTCA	55,9	45,5	153	2,005592239	
24.2 PHOT1_R	GGGAGTCCCATCCTTCTTGT	58,3	55			

Apart from TAC1, primer efficiencies were between the required (1,8 and 2,1) which was calculated by measuring the slope of the standard curve. The curve was drawn from cycle threshold (Ct) values of 4 technical replicates using 4 different cDNA dilutions. The slope was then uploaded on online qPCR efficiency calculator (Thermo Fisher: qPCR Efficiency). The efficiency calculation experiment was carried out according to the Roche LightCycler 480 SYBR Green I Master, version 13 protocol with following sample mix and settings: 88 µl of PCR grade water, 110 µl of 2x master mix, 11 µl of forward primer and 11 µl of reverse primer was mixed and kept on ice. The master mix was pipetted onto a well plate (9 µl per well) with 4 technical replicates per primer pair and dilution. Subsequently, 1 µl of 1/16, 1/32, 1/64 and 1/128 diluted cDNA was pipetted onto different sectors (A = 1/16, B = 1/32, C=1/64, D=1/128). qPCR –program was following: pre-incubation at 95°C for 10 min. Amplification 45 times at 95°C for 10 sec, at 58°C for 10 sec, at 72°C for 20 sec.

RT-qPCR experiment

RT-qPCR experiment was carried out by pipetting the master mix for each primer pair and then pipetting 1 µl of 1:7 (cDNA:H_2O) into the sample blocks. Two technical repeats were used per primer pair in each block. qPCR program was the same as in the efficiency calculation. Melt curve analysis was conducted with Bio-Rad CFX Maestro 1.1 v.4.1.2433. 1219. *ACTIN7*, one of the reference genes, had issues with product forming in the H_2O control (no cDNA template). Signal in the H_2O control was evident at Ct-value ~35 whereas the "main" signal was at Ct 25-27. Further melt curve and melt peak analysis (Fig 6) displayed that the products in the H_2O controls had lower melting temperatures. However, due to the much higher Ct value (~9) in the H_2O controls and its different melt peak value, *ACTIN7* was accepted as a reference gene. The additional signal it produces in the background should have very little effect on the fluorescence of the main signal. Ct-values were exported and results were normalized as described previously (Vandesompele *et al.,* 2002; Livak & Schmittgen, 2001; Smetana *et al.,* 2019).

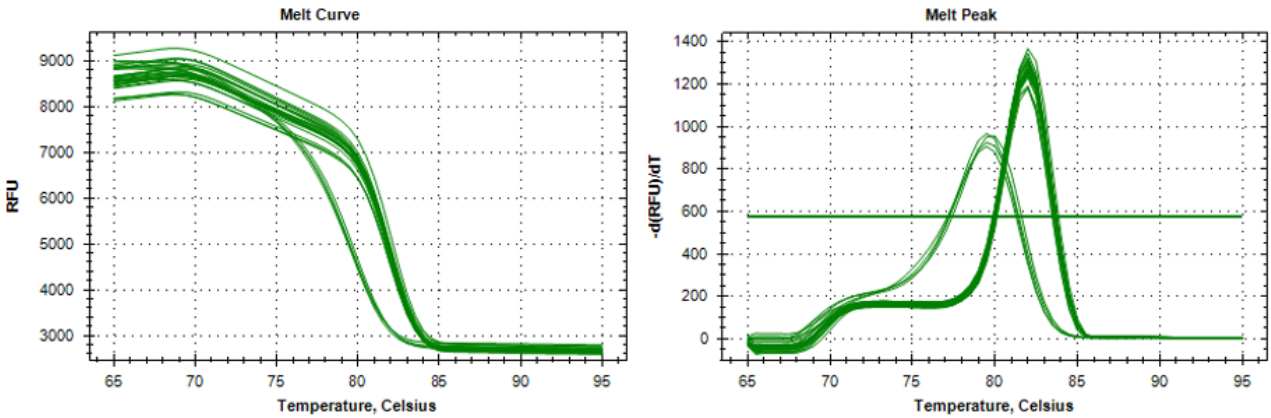

Figure 6. Melt curve and melt peak analysis of *ACTIN7* reference gene. Melt curve analysis indicates that there are two products. One of the products is losing fluorescence earlier than the main product indicating that there is an issue with purity or specificity of the primers.

3.6 Statistical Methods

All statistical analyses were conducted with SPSS v.24 except for the RT-qPCR experiment which was analyzed in Excel 2013. Statistical analysis used in each experiment is stated where appropriate.

4 RESULTS

4.1 Two distinct *LAZY1* genes in studied tree species

According to the LAZY phylogeny tree (Fig 7) and simplified (fewer genes) amino acid alignment (Fig 8), it is very likely that the tree species (*Betula pendula, Prunus persica, Populus trichocarpa*) compared in this alignment have a duplicated *LAZY1* gene. Finding the duplication in *Alnus glutinosa* genome is still underway. These duplicates fall into two distinct clades: *LAZY1a* and *LAZY1b*. When a BLAST search (www.phytozome.org) was conducted using either *Betula pendula LAZY1a* or *LAZY1b* gene, the best match was *LAZY1* in *Arabidopsis thaliana*. When the same search was conducted against the studied tree species, best hits were two different genes *LAZY1a* and *LAZY1b*, respectively. In *Arabidopsis thaliana, Oryza sativa* and *Zostera marina*, the second copy of *LAZY1* is absent.

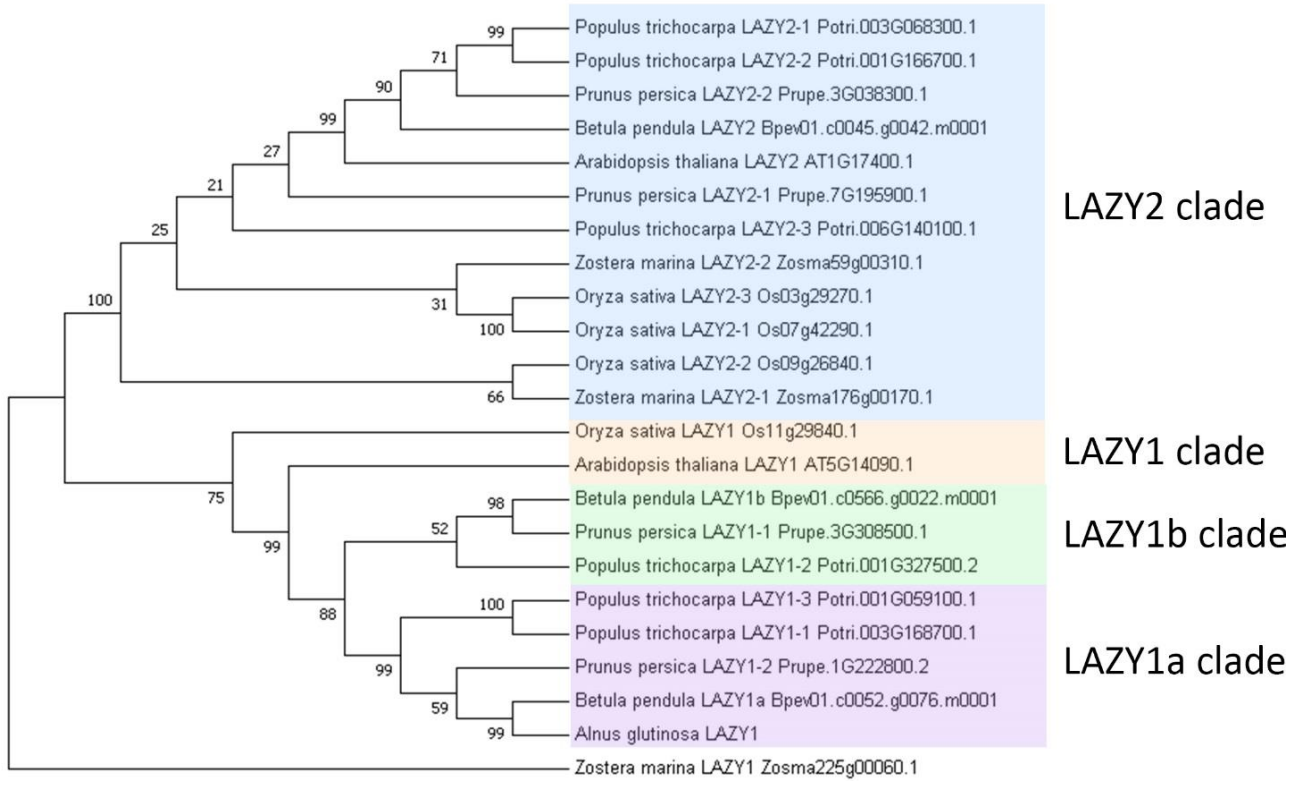

Figure 7. Molecular Phylogenetic Analysis by Maximum Likelihood Method. Closest matches of *Betula pendula* LAZY1a paralogs in different tree species forms a distinct LAZY1a clade. The studied tree species also contain LAZY1b clade. In contrast, *Arabidopsis thaliana*, *Oryza sativa* and *Zostera marina* contain only a single *LAZY1* gene. *Zostera marina* LAZY1 was employed as the root of the phylogenetic tree.

4.2 Simplified LAZY1, LAZY1a, LAZY1b and LAZY2 Protein Sequence Alignment

Simplified multiple protein sequence alignment (Fig 8) provided evidence of 3 conserved domains among all studied species in *LAZY1*, *LAZY1a*, *LAZY1b* and *LAZY2* genes. The *LAZY*-clade has been previously linked to the IGT gene family due to the highly conserved IGT motif (Dardick *et al*., 2013). In this alignment the IGT motif is in domain 1. Although *LAZY1* gene has been studied extensively in recent times, its molecular function remains unknown. The Pfam protein function database (https://pfam.xfam.org) did not provide any predicted function when *LAZY1a* sequence was used to find matching Pfam entries.

4.3 *LAZY1a* and *LAZY1b* Expression Pattern in *B. pendula*

Data extracted from *B. pendula* fractional RNA-sequence analysis (Alonso-Serra *et al.,* 2019) provided evidence that the expression pattern of *LAZY1a* and *LAZY1b* is highly similar peaking in old phloem (Fig 9). To study whether their function is also redundant, one should generate single and double knock-out lines and compare whether double knock-out line has cumulative effect on the phenotype.

One could speculate that since *LAZY1a* and *LAZY1b* genes are tree specific, they might have distinct function in primary and secondary growth. According to Gerttula *et al.* (2015), in Poplar stem the gravity perceiving cells, statocytes, are first observed in the innermost layer of cortex. After the loss of this layer, statocytes are observed in the secondary phloem. Perhaps, *LAZY1a* and *LAZY1b* have role in this spatial difference since *LAZY1* is known to be expressed in *Arabidopsis* statocytes (Taniguchi *et al*., 2017). One could study this by generating *LAZY1a* and *LAZY1b* promoter-GFP-tag analysis, in a tree species.

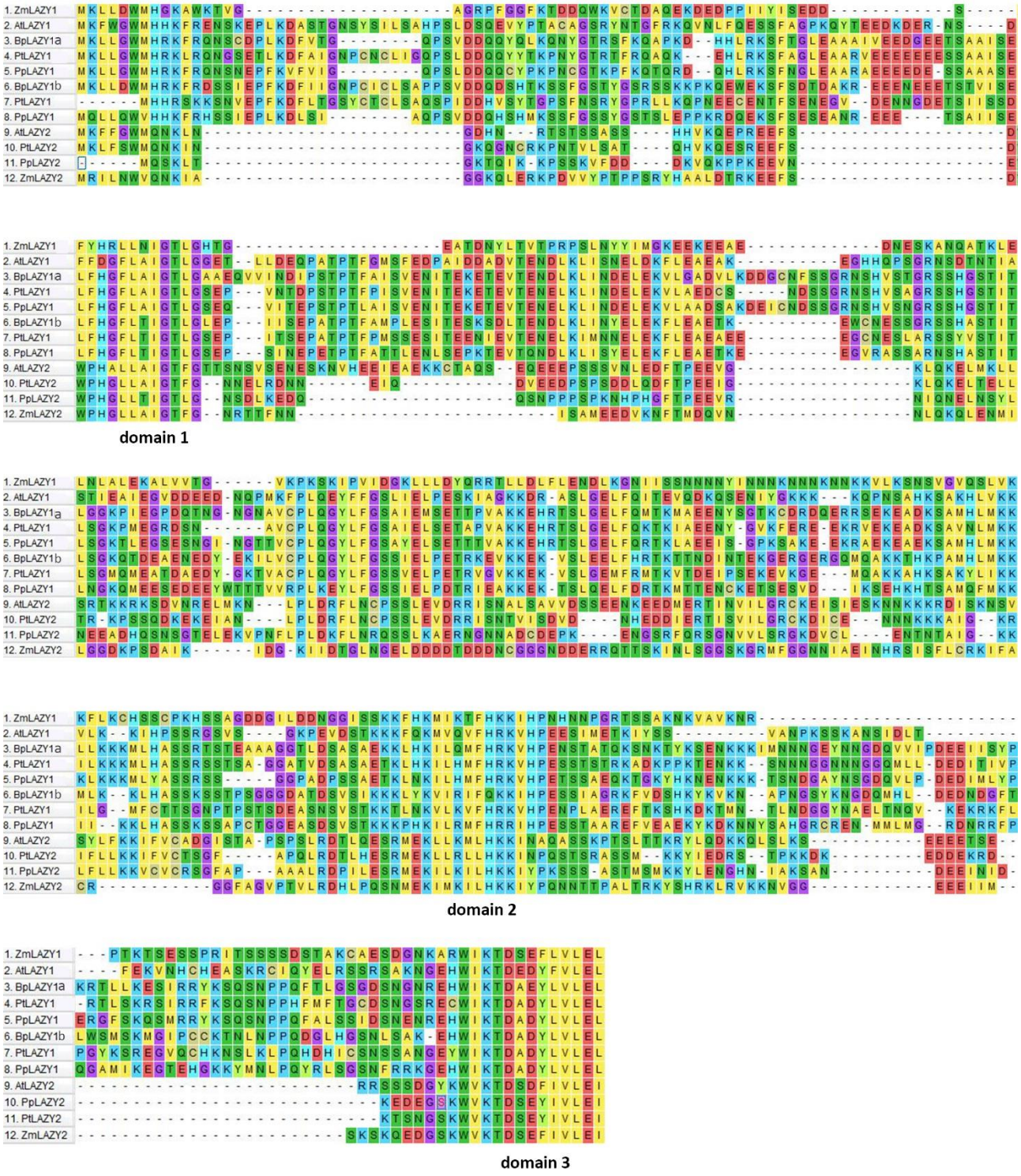

Figure 8. Simplified alignment map of the sequences employed to construct the phylogenetic tree (Fig 7). Zm = *Zostera marina*, At = *Arabidopsis thaliana*, Bp = *Betula pendula*, Pt = *Populus trichocarpa*, Pp = *Prunus persica*. All studied sequences share three highly conserved domains. To date, the molecular function of *LAZY* genes remains unknown.

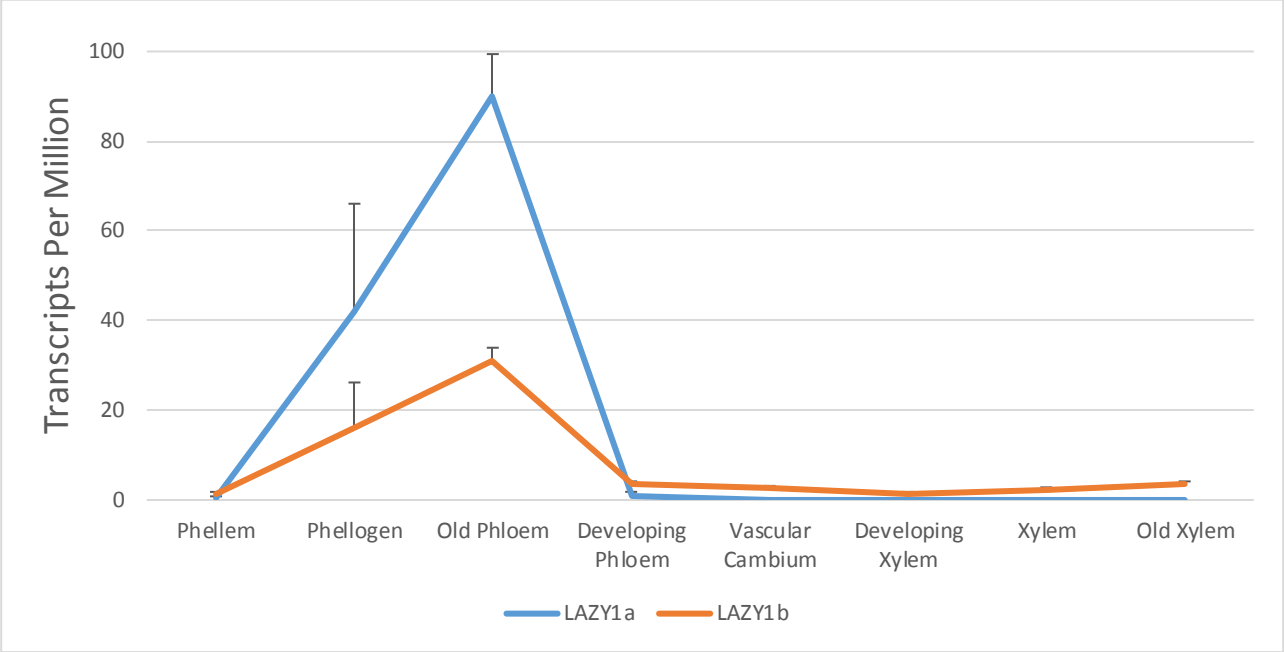

Figure 9. *LAZY1a* and *LAZY1b* gene expression pattern in *Betula pendula*. Data extracted from silver birch RNA-seq analysis (Alonso-Serra et al., 2019) provided evidence that *LAZY1a* and *LAZY1b* are redundantly expressed mainly in old phloem. Error bars ±1 STD.

4.4 Two Branch Angle Phenotypes in the Segregating Population

LAZY1 has been previously reported to regulate shoot orientation in poplar (Populus × zhaiguanheibaiyang). 35S:Pzlazy1 over expression construct resulted in trees with narrower branch angle compared to wild type trees (Xu *et al.* 2017; Hollender and Hill 2019). Further, *LAZY1* RNAi knockdown plum trees had wider branch angles compared to wild type trees, and they also displayed pendulous growth (Hollender and Hill, 2019). These data are in line with results presented here. Visual branch angle analysis indicated that there might be 3 different branch angle phenotypes in the segregating population (Fig 10). Mixed linear model was employed to analyze data from 3 wild type (66 branches), 3 intermediate (68 branches) and 3 mutant (68 branches) phenotype trees. The analysis provided evidence that *lazy1a* phenotype has wider branch angle compared to the wild type (Fig 11). The difference was not large but still it was significant (P-value 0,044). Wild type was not significantly different from the intermediate phenotype.

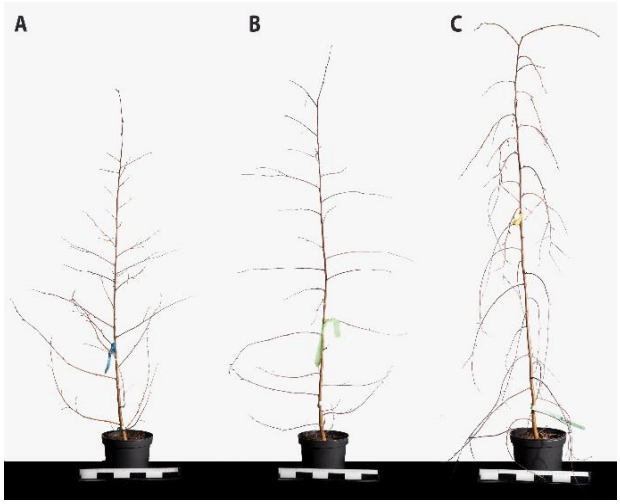

Figure 10. Presumed branch angle phenotypes in the segregating population. **(A)** wild type **(B)** intermediate **(C)** mutant.

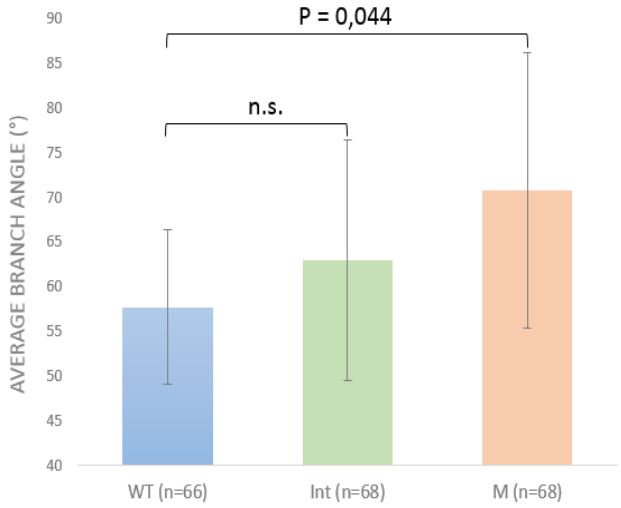

Figure 11. Two branch angle phenotypes in the segregating population. Mixed linear models analysis provided evidence that there are only two different branch angle phenotypes in the segregating population.

4.5 Adaxial and Abaxial Fiber Lengths Similar in Both Phenotypes

Samples for fiber length analysis were sectioned from the indicated positions from 5 wild type and 5 mutant trees (Fig 12). Fiber length measurements indicated that adaxial and abaxial xylem fiber lengths are not significantly different in wild type vs. mutant (Figure 13). Thus, the weeping phenotype is probably not due to differential fiber elongation on upper vs. lower side of the branches.

Figure 12. 5 wild type and 5 mutant trees used in fiber length analysis. Blue arrows indicate regions which were sectioned for maceration.

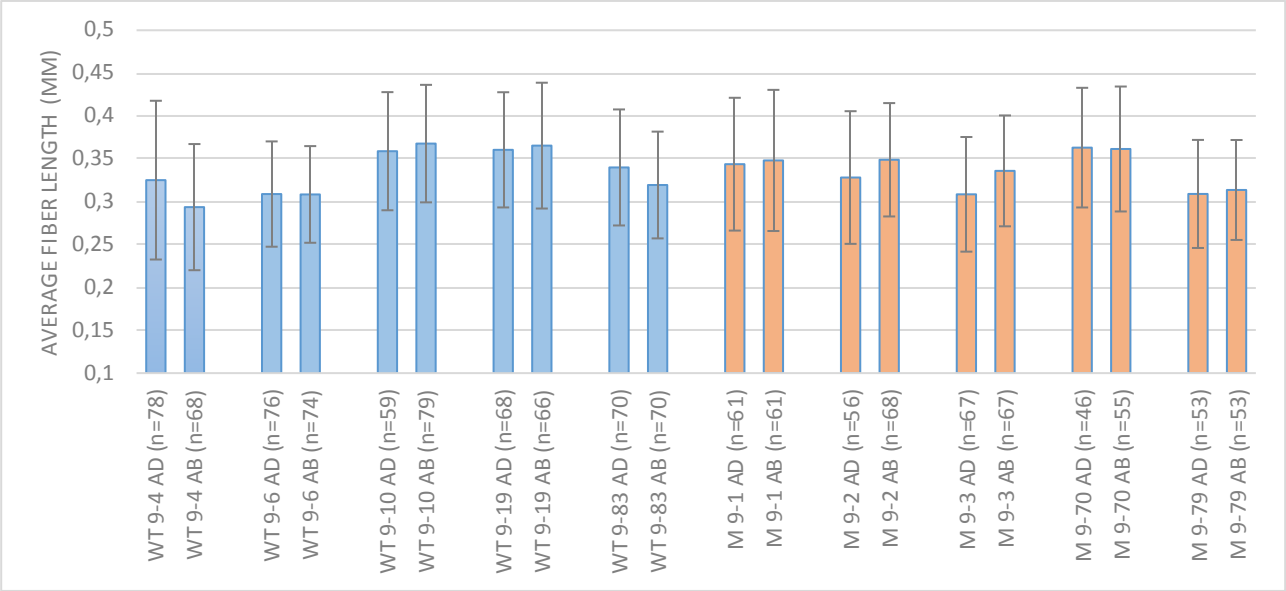

Figure 13. Average fiber lengths measured from macerated adaxial and abaxial branch sections. Pairwise t-test analysis indicated that **a**daxial and abaxial fiber lengths are not significantly different when comparing upper fibers to lower fibers within the biological sample. Error bars ±1 STD.

4.6 Abnormal Reaction Wood Formation in Wild Type and Mutant Branches

Tension wood is ought to form on the upper side of stems and branches in angiosperm trees creating a tensile force that pulls stem away from gravity vector. A main hypothesis in this project was that the weeping phenotype of ´Youngii´ birch is due to lack of or erratic tension wood deposition. In the studied samples tension wood was always observed among thick walled and heavily lignified cells. This made image quantification very problematic because some of the Alcian Blue (carbohydrate binding) signal might be lost due to heavy Safranin (lignin binding) staining. Also, because G-layers are not covalently bonded to the surrounding cell walls (Barnett *et al.,* 2014: 8), it is problematic to employ cryo-sectioned and stained images as evidence of tension wood deposition. G-layers might detach from surrounding cell walls while preparing sections for imaging. Therefore, one cannot objectively analyze from bright field microscopic images what kind of cell wall structure there is in the densely stained regions (Figures 14-17). For this reason, the images are analyzed qualitatively and tension wood is called here as reaction wood (RW).

A section from a wild type tree (Fig 14) displays an expected RW deposition pattern where RW is formed on top of the branch. However, a section taken from the same branch 10 cm before (Fig 15) displays a ring-like RW pattern: RW is deposited around the xylem and not on the top, as expected. Similar RW deposition was also observed in *lazy1a* mutants. RW was observed but G-layers were

not evident in a sample which was sectioned 21 cm from the base of the branch (Fig 16A). But when the same branch was observed closer to the stem (11 cm), some G-layers were observed and a fan-like formation of thick-walled RW was evident (Fig 17).

Due to the subjective nature of identifying tension wood within the samples, a qualitative analysis of reaction wood deposition was conducted. A density map of reaction wood occurrence was created by fitting all imaged samples (18 wild type and 18 mutant) within a circle. Normal wood was then removed from the images in Photoshop, then colored blue and transparency set to 5%. The resulting density map (Fig 18) provides qualitative evidence that reaction wood is deposited rather evenly around the branch xylem. It seems that wild type displays more reaction wood on top of the branch but one would need more objective method to confirm this.

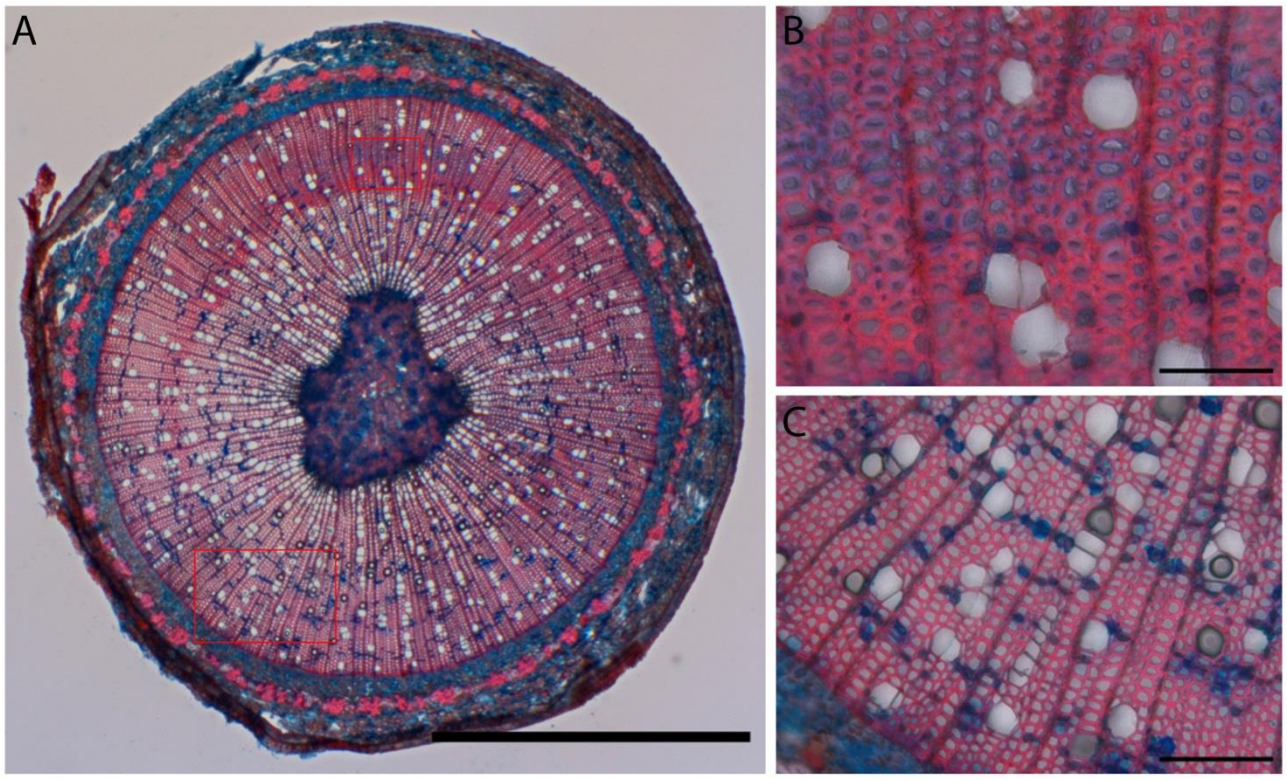

Figure 14. Wild type #9-10. 21 cm from the stem. **(A)** Tension wood deposition as expected in wild type branch. G-layers are deposited on top of the branch possibly affecting the direction of branch growth. Scale bars: **A** 1 mm, **B** 5 um, **C** 10 um.

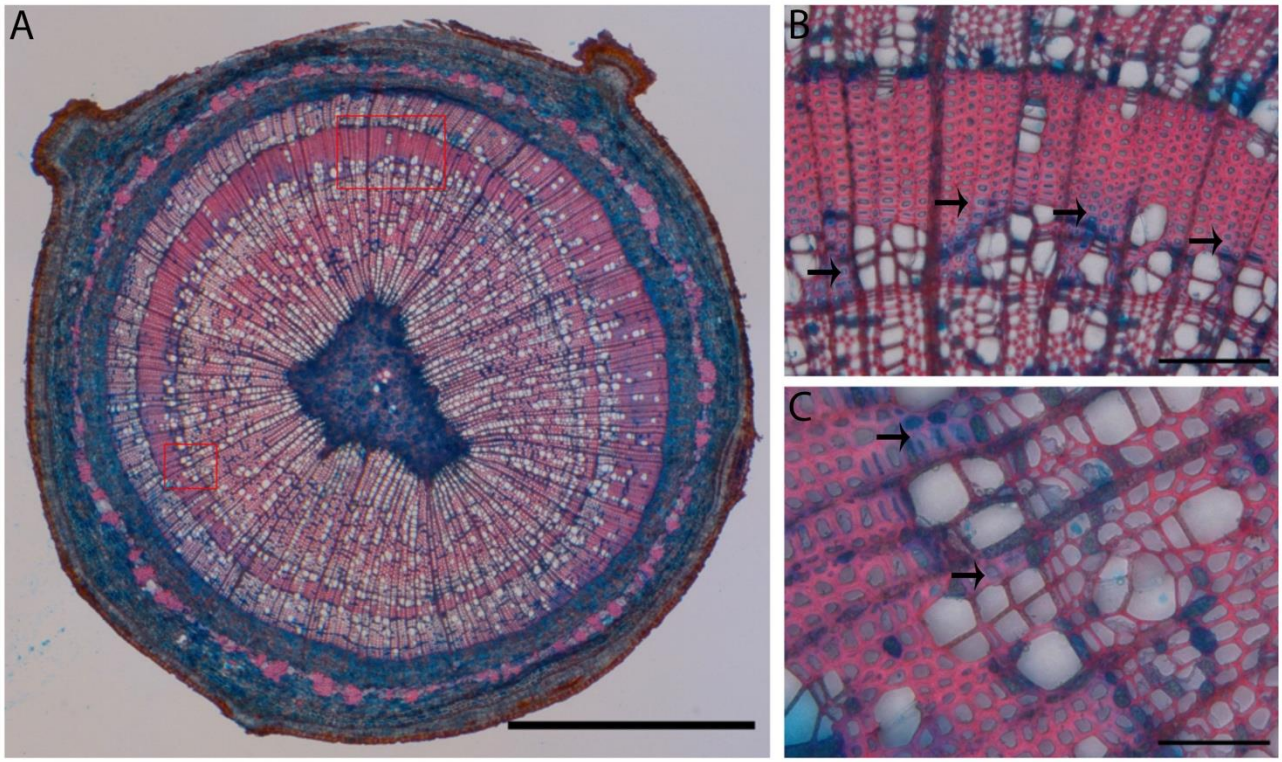

Figure 15. Wild type #9-10. 11 cm from the stem. **(A)** Section sampled from the same branch as in Figure 14 but 10 cm closer to the stem. Reaction wood and G-layers are deposited around the section. Arrows indicate G-layers. Scale bars: (**A)** 1 mm, (**B)** 10 um, (**C)** 5 um.

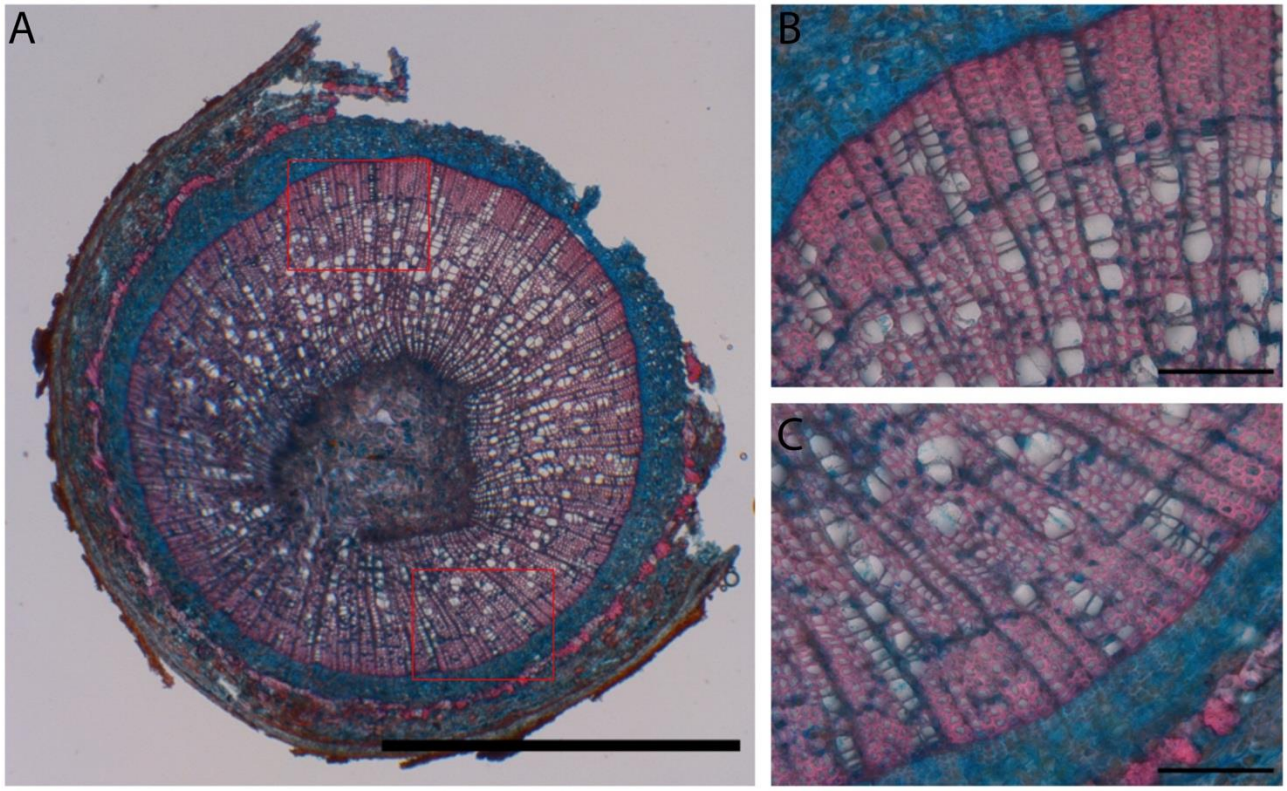

Figure 16. Mutant #9-70. 21 cm from the stem. Section sampled from a mutant branch displays a ring like formation of reaction wood at the xylem periphery. No G-layers were evident. Scale bars: **A** 1 mm, **B** 10 um, **C** 10 um.

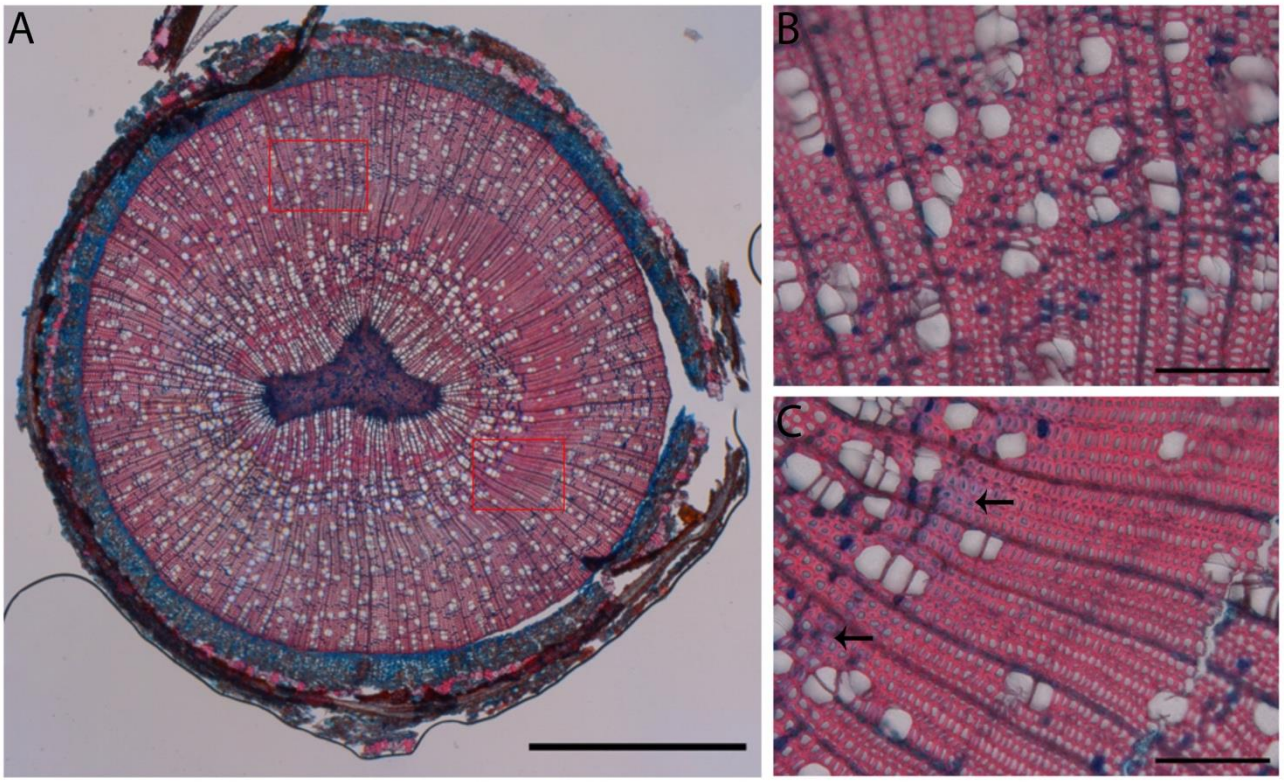

Figure 17. Mutant #9-70. 11 cm from the stem. **(A) S**ection sampled from a mutant branch displays a fan like reaction wood deposition. **(B)** Normal wood on the upper flank of the branch. **(C)** Some G-layer clusters observed (indicated with arrows). Scale bars: **A** 1 mm, **B** 10 um, **C** 10 um.

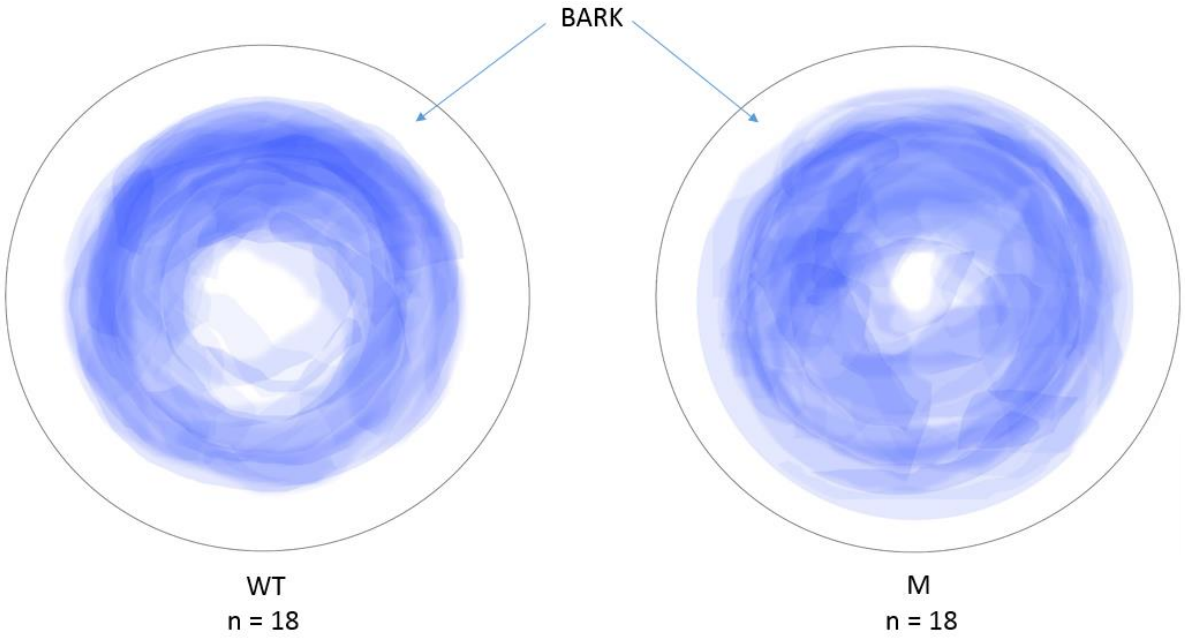

Figure 18. Reaction wood density maps constructed from 18 wild type and 18 mutant branch sections. Cryo-sectioned **s**amples were stained with Alcian Blue and Safranin. Samples were imaged and Photoshop was used to erase normal wood. The darker the blue, the more frequently reaction wood was observed. Results are not quantitative because of uncertainty in image based analysis – G-layered tension wood could not always be distinguished from thick walled reaction wood.

4.7 *LAZY1a* Transcript Levels Higher in Wild Type Compared to Mutant

Gene expression analysis by RT-qPCR indicated that *LAZY1a* transcript levels are significantly higher (p-value 0,03) in wild type top flank vs. mutant top flank (Fig 19). Same comparison of *LAZY1a* in bottom flanks was close to being significant (p-value 0,05). *ARK2*, *ARF_19*, *WOX4*, *PIN3* or *PHOT1* did not display varying expression in wild type vs. mutant. *LAZY1b* primers did not amplify the appropriate sequence and it was therefore excluded from the experiment.

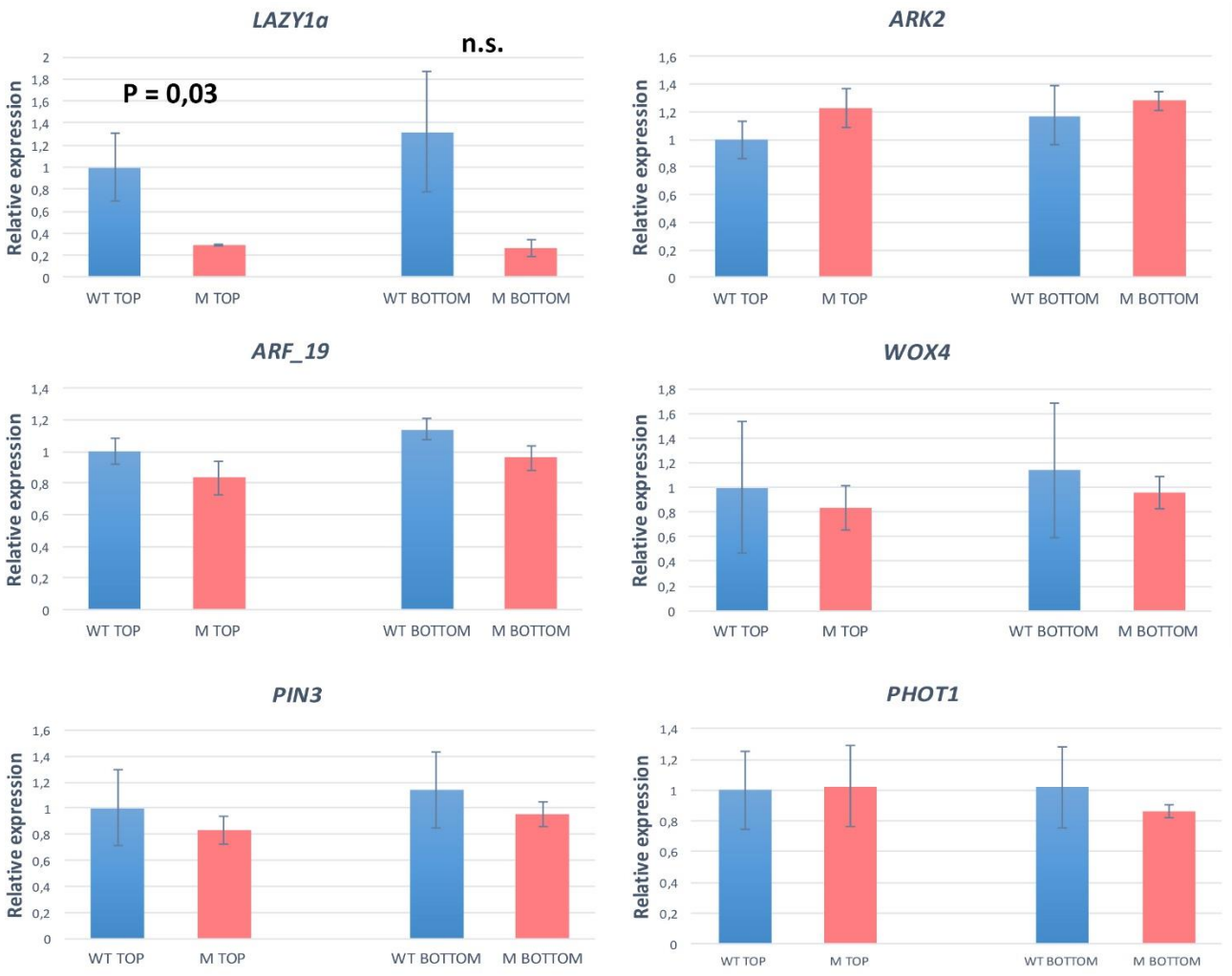

Figure 19. Transcript levels of candidate genes analyzed by RT-qPCR from three biological replicates. Pairwise t-test analysis indicated that only *LAZY1a* transcript levels were significantly higher in WT top vs. M top (p-value 0,03). WT bottom vs. M bottom was close to being significant (p-value 0,05). Other measured transcript levels were not significantly different in WT vs. M. Error bars ±1 STD.

5 DISCUSSION

Function of *LAZY1* has been studied extensively due to its importance in agriculture and fruit production. Despite the research efforts, molecular function of *LAZY1* remains elusive. Thus, there is still a crucial knowledge gap between amyloplast sedimentation and subsequent reorientation of growth direction (Hollender *et al.,* 2019).

The phylogenetic tree of *LAZY1*, *LAZY1a*, *LAZY1b* and *LAZY2* provided evidence that the studied tree species (*Betula pendula, Prunus persica, Populus trichocarpa*) have at least one duplicated *LAZY1* gene and they fall into two clades: *LAZY1a* and *LAZY1b*. *Alnus glutinosa* and *A. incana* genomes are currently being investigated for the duplication. However, it is likely that they also have the second copy of *LAZY1* due to their proximity to *Betula* species. In *Arabidopsis thaliana, Oryza sativa* and *Zostera marina*, the second copy of *LAZY1* was absent. It could be potentially rewarding to study whether LAZY1a and LAZY1b have redundant or distinct function in tree species. This could be executed by generating single and double knock-out lines. By phenotyping these lines one could possibly detect whether the double knock-out line has cumulative effect on the weeping phenotype. Also, RNA-sequence data from *B. pendula* displayed that the expression pattern of *LAZY1a* and *LAZY1b* is similar. One could devise a promoter-reporter experiment to study with better resolution if *LAZY1a* and *LAZY1b* expression is spatially distinct. If *LAZY1b* has more minor impact on branch angle than *LAZY1a*, it might provide a good knock-out target for tree breeding, since the optimal (horizontal) branch angle for timber production is somewhere between the wild type and *lazy1a* mutant.

According to Barnett *et al*. (2014: 2-3), reaction wood is not bending branches into a stem-like upward growth unless apical dominance is gone. This suggests some overriding mechanism that takes place in tension wood deposition (or quality) in branches when the shoot apical meristem is lost. Also, it has been reported that in stems of intensively growing hybrid aspens tension wood is scattered randomly around stem sections, indicating a role of stress in tension wood induction (Barnett *et al.,* 2014: 3). As branches are growing more or less horizontally compared to the stem, there are different stress factors affecting the maturing fibers in branches. This might explain the observed rather evenly distributed reaction wood in both wild type and mutant branches. Another possible explanation for highly lignified cell walls in the observed samples is that some of the G-

layers are lignified during maturation. Similar phenomena have been described in tropical angiosperm species *Simarouba amara* by Roussel & Clair (2015). According to their observation, in some instances the G-layer is only a temporary phase and is later lignified. This issue could be possibly averted if there was fresh plant material to study. Sections should be made during very early phase when the weeping phenotype becomes evident. In this project however, this would have been impossible due to the problems in *in vitro* propagation.

It is problematic to study tension wood deposition by studying stained histological samples due to difficulties in separating thick walled reaction wood from G-layers. However, this study has provided important knowledge on how one could proceed with tension wood analysis. Chemical analysis of total cellulose content in upper vs. lower flanks of branches combined with stained sections could provide a more objective method to evaluate tension wood quantity.

LAZY1a transcript levels were significantly higher in wild type compared to mutant. This is probably due to the pre-mature stop codon in the *lazy1a* transcript. Pre-mature stop codons are recognized in eukaryotes by nonsense-mediated mRNA decay (NMD) and subsequently these transcripts are degraded (Shi *et al.,* 2015). Other transcripts that were successfully analyzed did not have significant difference in their expression levels. For future analysis, one should conduct RNA-sequencing to analyze the effect of *lazy1a* mutation in the silver birch transcriptome. Also, it would be important to analyze transcript levels of both *LAZY1a* and *LAZY1b* in wild type vs. *lazy1a* mutant.

During the ´Youngii´ project it was discovered that the *lazy1a* birches display very poor root growth in *in vitro* propagation making cloning virtually impossible. It could be potentially very interesting to study by RT-qPCR, whether silver birch has *LAZY1a* and/or *LAZY1b* expression in root tips and whether this might affect root growth. As indicated by Taniguchi *et al.* (2017), *LAZY1* is not expressed in the root tips in *Arabidopsis*. Perhaps in woody plants *LAZY1a* and/or *LAZY1b* has significant role also in the root system.

It has been demonstrated that effective tensional force generation in wood fibers requires microfibril angle less than 10° (Wahyudi *et al.,* 2000; Fagerstedt *et al.,* 2014). The reason why no clear phenotype was seen in this project might be due to the smaller scale changes that occur in plant cell walls. Cortical microtubules and, hence, cellulose microfibril biosynthesis have been

demonstrated to reorient from transversal to longitudinal in epidermis of *Arabidopsis* root and hypocotyl by auxin treatment (reviewed by Eoda, 2015). Perhaps, there is ill orientation of cellulose microfibrils in *lazy1a* which affects the tensional stress that cells are able to project to adjacent cells. In future studies, orientation of cellulose microfibrils should be studied by X-ray diffraction.

AKNOWLEDGEMENTS

I want to thank especially the closest supervisors of this project: Professor Ykä Helariutta, Dr. Kaisa Nieminen and Juan Alonso Serra. Juan´s persistent support and guidance in various methods and data handling aided immensely in taking this project through its stages from ideas to execution of experiments. Special gratitude goes also to the whole tree team that has given invaluable feedback throughout the project: Su Chang, Dr. Juha Immanen and Dr. Melis Kucukoglu.

REFERENCES

Alonso-Serra, J., Safronov, O. & Lim, K-J. *et al.* (2019). Tissue-specific study across the stem reveals the chemistry and transcriptome dynamics of birch bark. *New Phytologist*. 222(4), pp. 1816-1831.

Arsuffi, G & Braybrook, S. (2018). Acid growth: An ongoing trip. *Journal of Experimental Botany.* 69(2), pp. 137-146.

Ashburner, K., McAllister, H.A. & Rix, M. (2013). *The Genus Betula: A Taxonomic Revision of Birches*. Royal Botanic Gardens.

Barnett, J. R. & Jeronimidis, G. (eds.). (2003). *Wood Quality and its Biological Basis*. Oxford: Blackwell Publishing.

Barnett, J., Saranpää, P., Gril, J. & Gardiner, B. (eds.). (2014). *The Biology of Reaction Wood*. Heidelberg: Springer.

Björklund, S., Antti, H., Uddestrand, I., Moritz, T., Sundberg, B. (2007). Cross-talk between gibberellin and auxin in development of Populus wood: Gibberellin stimulates polar auxin transport and has a common transcriptome with auxin. *Plant Journal, 52*(3), pp. 499-511.

Cernansky, R. (2018). How to plant a trillion trees. *Nature,* 560(7720), pp. 542-544.

Christie, J., Salomon, M., Nozue, K., Wada, M., Briggs, W. (1999). LOV (light, oxygen, or voltage) domains of the blue-light photoreceptor phototropin (nph1): Binding sites for the chromophore flavin mononucleotide. *Proceedings of the National Academy of Sciences of the United States of America, 96*(15), pp. 8779-8783.

Dardick, C., Callahan, A., Horn, R., Ruiz, K., Zhebentyayeva, T., Hollender, C., Whitaker, M., Abbott, A., Scorza, R. (2013). PpeTAC1 promotes the horizontal growth of branches in peach trees and is a member of a functionally conserved gene family found in diverse plants species. *Plant Journal, 75*(4), pp. 618-630.

Du, S. & Yamamoto, F. (2007). An Overview of the Biology of Reaction Wood Formation. *Journal of Integrative Plant Biology, 49*(2), pp. 131-143.

Eoda, Y. (2015). Cortical microtubule rearrangements and cell wall patterning. *Frontiers in Plant Science, 6*. doi:10.3389/fpls.2015.00236

Fagerstedt K., V., Mellerowicz, E., Gorshkova, T., Ruel, K., Joseleau, J-P. (2014). in *The biology of reaction wood*. Heidelberg: Springer.

Foley, J. A., Ramankutty, N., Brauman, K., Gerber, J., Johnston, M., Mueller N., O'connell, C., Deepak K., ; West, P., Balzer, C., Bennett, E., Carpenter, S., Hill, J., Monfreda, C., Polasky, s., Rockström, J., Sheehan, J., Siebert, S., Tilman, D., Zaks D. (2011). Solutions for a cultivated planet. *Nature, 478*(7369), p. 337.

Friml, J., Wiśniewska, J., Benková, E., Mendgen, K., and Palme, K. (2002). Lateral relocation of auxin efflux regulator PIN3 mediates tropism in Arabidopsis. *Nature,* 415(6873), pp. 806–809.

Fukaki, H., Wysocka-Diller, J., Kato, T., Fujisawa, H., Benfey, P., Tasaka, M. (1998). Genetic evidence that the endodermis is essential for shoot gravitropism in Arabidopsis thaliana. *Plant Journal, 14*(4), pp. 425-430.

Gerttula, S., Zinkgraf, M, Muday, G. K., Lewis, D. R.,Ibatullin, F., Brumer, H., Hart, F., Mansfield, S. D., Filkov, V., Groover, A. (2015). Transcriptional and hormonal regulation of gravitropism of woody stems in populus. *Plant Cell, 27*(10), pp. 2800-2813.

Gril, J. Jullien, D., Bardet, S., Yamamoto, H. (2017). Tree growth stress and related problems. *Journal of Wood Science, 63*(5), pp. 411-432.

Haberlandt, G. (1900). Uber die Perzeption des geotropischen Reizes. *Ber. Dtsch. Bot. Ges.* 18: 261–272.

Hill, J. & Hollender, C. (2019). Branching out: New insights into the genetic regulation of shoot architecture in trees. *Current Opinion in Plant Biology, 47*, pp. 73-80.

Hollender, C. A., Pascal, T., Tabb, A., Hadiarto, T., Srinivasan, C., Wang, W., Liu, Z., Scorza, R., Dardick, C. (2018). Loss of a highly conserved sterile alpha motif domain gene (WEEP) results in pendulous branch growth in peach trees. (PLANT BIOLOGY). *Proceedings of the National Academy of Sciences of the United States, 115*(20), p. E4690.

Immanen, J., Nieminen, K., Smolander, O-P., Kojima, M., Alonso serra, J., Koskinen, P., Zhang, J., Elo, A., Mähönen, AP., Street, N., Bhalerao, R., Paulin, L., Auvinen, P., Sakakibara, H, Helariutta, Y. 2016. Cytokinin and Auxin Display Distinct but Interconnected Distribution and Signaling Profiles to Stimulate Cambial Activity. *Current Biology, 26*(15), pp. 1990-1997.

IPCC (2018) Global Warming of 1.5°C. Headline Statements from the Summary for Policymakers. https://www.ipcc.ch/site/assets/uploads/sites/2/2018/07/sr15_headline_statements.pdf. Accessed 5.12.2018.

Jacob, H. (2010). Breeding Experiments of Apple Varieties with Columnar Growth and Low Chilling Requirements. *Acta horticulturae, 872*, pp. 159-164.

Kumar, S., Stecher, G., Tamura, K. (2015) MEGA7: Molecular Evolutionary Genetics Analysis version 7.0. Molecular Biology and Evolution

Li, P., Wang, Y., Qian, Q., Zhiming, F., Mei, W., Dali, Z., Baohua, L., Xiujie, W., Jiayang, L. (2007). LAZY1 controls rice shoot gravitropism through regulating polar auxin transport. *Cell Research, 17*(5), p. 402.

Longman, K. A. & Wareing, P.F. (1959). Early Induction of Flowering in Birch Seedlings. *Nature, 184*(4704), p. 2037.

Mann, C., & Plummer, M. (2002). Forest biotech edges out of the lab. *Science, 295*(5560), p. 1626.

Mellerowicz, E. & Gorshkova, T. (2011). Tension stress generation in gelatinous fibres: A review and possible mechanism based on cell-wall structure and composition. *Journal Of Experimental Botany, 38*(4), pp. 111-122.

Ming, R. & Man Wai, C. (2015). Assembling allopolyploid genomes: No longer formidable. *Genome Biology, 16*(1).

Moyle, R., Schrader, J Stenberg, A., Olsson, O., Saxena, S., Sandberg, G., Bhalerao, R.P. (2002). Environmental and auxin regulation of wood formation involves members of the Aux/IAA gene family in hybrid aspen. *Plant Journal, 31*(6), pp. 675-685.

Nilsson, J., Karlberg, A., Antti, H., Lopez-Vernaza, M., Mellerowicz, E., Perrot-Rechenmann, C., Sandberg, G., Bhalerao, R. (2008). Dissecting the molecular basis of the regulation of wood formation by auxin in hybrid aspen. *Plant Cell, 20*(4), pp. 843-855.

Niemistö, P. (2008). *Koivun kasvatus ja käyttö*. Helsinki: Metsäkustannus, Metla.

Roussel, J-R. & Clair, B. (2015). Evidence of the late lignification of the G-layer in Simarouba tension wood, to assist understanding how non-G-layer species produce tensile stress. *Tree Physiology, 35*(12), pp. 1366-1377. doi:10.1093/treephys/tpv082

Ruelle, J. (2014) in *The biology of reaction wood*. Heidelberg: Springer.

Salojärvi, J. et al. (2017). Genome sequencing and population genomic analyses provide insights into the adaptive landscape of silver birch. *Nature Genetics, 49*(6).

Sutela, S., Niemi, K., Edesi, J., Laakso, T.,Saranpää, P., Vuosku, J., Mäkelä, R., Tiimonen, H., Chiang, V.L., Koskimäki, J., Suorsa, M., Julkunen-Tiitto, R., Häggman, H. (2011). Phenolic compounds in ectomycorrhizal interaction of lignin modified silver birch. *Acta Veterinaria Scandinavica, 53*(1)

Livak & Schmittgen. (2001). Analysis of relative gene expression data using real-time quantitative PCR and the 2−ΔΔCT method. *Methods,* 25, pp. 402–408

Shi, M. (2015). Premature termination codons are recognized in the nucleus in a reading-frame-dependent manner. *Cell Discovery, 1*(1).

Suer, S. Agusti, J., Sanchez, P., Schwarz, M., Greb, T. (2011). WOX4 Imparts Auxin Responsiveness to Cambium Cells in Arabidopsis. *The Plant Cell, 23*(9), pp. 3247-3259.

Taniguchi, M.,Furutani, M., Nishimura, T., Nakamura, M., Fushita, T., Iijima, K., Baba, K., Tanaka, H., Toyota, M., Tasaka, M., Morita, M.T. (2017). The Arabidopsis LAZY1 Family Plays a Key Role in Gravity Signaling within Statocytes and in Branch Angle Control of Roots and Shoots. *The Plant cell, 29*, p. 1984.

Tocquard, K., Lopez, D., Decourteix, M., Thibaut, B., Julien, J-L., Label, P., Leblanc-Fournier, N., Roeckel-Drevet, P. (2014). *The biology of reaction wood*. Heidelberg: Springer.

Untergasser, A., Nijveen, N., Rao, X., Bisseling, T., Geurts, R. & Leunissen J. (2007). Primer3Plus, an enhanced web interface to Primer3 Nucleic Acids Research, 35: 71-74.

Vandesompele, J. et al. (2002). Accurate normalization of real-time quantitative RT-PCR data by geometric averaging of multiple internal control genes. Genome Biol. 3.

Wahyudi I, Okuyama T, Hadi YS, Yamamoto H, Yoshida M, Watanabe H. (2000). Relationship between growth rate and growth stresses in Paraserianthes falcataria grown in Indonesia. *Journal of Tropical Forest Products,* 6:95–105.

Xu, D., Xiao, Q., Jihong, K., Xiaojiao, H., Jinnan, W., Yuezhong, J., Yanting, T., Yiwei, W. (2017). PzTAC and PzLAZY from a narrow-crown poplar contribute to regulation of branch angles. *Plant Physiology and Biochemistry, 118*, pp. 571-578.